THE JOURNAL OF COMPARATIVE NEUROLOGY 435:291–310 (2001)

Thalamo-Cortical Connections of Areas 3a and M1 in Marmoset Monkeys

KELLY J. HUFFMAN AND LEAH KRUBITZER
Center for Neuroscience and Department of Psychology, University of California, Davis, Davis, California 95616

ABSTRACT

The present investigation is part of a broader effort to examine cortical areas that contribute to manual dexterity, reaching, and grasping. In this study we examine the thalamic connections of electrophysiologically defined regions in area 3a and architectonically defined primary motor cortex (M1). Our studies demonstrate that area 3a receives input from nuclei associated with the somatosensory system: the superior, inferior, and lateral divisions of the ventral posterior complex (VPs, VPi, and VPl, respectively). Surprisingly, area 3a receives the majority of its input from thalamic nuclei associated with the motor system, posterior division of the ventral lateral nucleus of the thalamus (VL), the mediodorsal nucleus (MD), and intralaminar nuclei including the central lateral nucleus (CL) and the centre median nucleus (CM). In addition, sparse but consistent projections to area 3a are from the anterior pulvinar (Pla). Projections from the thalamus to the cortex immediately rostral to area 3a, in the architectonically defined M1, are predominantly from VL, VA, CL, and MD. There is a conspicuous absence of inputs from the nuclei associated with processing somatic inputs (VP complex). Our results indicate that area 3a is much like a motor area, in part because of its substantial connections with motor nuclei of the thalamus and motor areas of the neocortex (Huffman et al. [2000] Soc. Neurosci. Abstr. 25:1116). The indirect input from the cerebellum and basal ganglia via the ventral lateral nucleus of the thalamus supports its role in proprioception. Furthermore, the presence of input from somatosensory thalamic nuclei suggests that it plays an important role in somatosensory and motor integration. J. Comp. Neurol. 435:291–310, 2001.

Indexing terms: primary motor cortex; somatosensory cortex; primates; ventral posterior nucleus; thalamus

The organization and connections of anterior parietal somatosensory cortical areas such as 3b, 1, and 2 have been well studied in primates (Kaas et al., 1979; Nelson et al., 1980; Sur et al., 1980; Pons et al., 1985; for review, see Kaas and Pons, 1988; Johnson, 1990). Areas 3b and 1 receive input from low-threshold mechanoreceptors and cutaneous receptors primarily via the ventral posterior nucleus of the dorsal thalamus, whereas area 2 receives inputs predominantly from muscle and joint receptors, as well as some cutaneous receptors via the ventral posterior superior nucleus and the anterior pulvinar nucleus of the dorsal thalamus (Nelson and Kaas, 1981; Pons and Kaas, 1985; for review, see Kaas and Pons, 1988). Although area 3a, which is also in the anterior parietal cortex, has been implicated in complex abilities such as sensorimotor integration and proprioception (Yumiya et al., 1974; Tanji, 1975; Guldin et al., 1992; for review, see Jones and Porter, 1980), relatively little is known about its organization and connections in primates. Indeed, most anatomical studies have focused on how areas 3b, 1, and 2 are interconnected with each other and with thalamic nuclei associated primarily with somatic processing. However, the somatosensory system must be tightly linked with the motor system to generate discrete, coordinated movements necessary for fine tactile discrimination, hand/mouth coordination, and goal-directed reaching. Area 3a, which receives most of its afferent input from muscle spindles (Oscarsson and Rosen, 1966; Landgren and Silfvenious, 1969; Phillips et al., 1971; Heath et al., 1976; Hore et al., 1976) and from

Grant sponsor: NIH; Grant number: 1 RO1 NS35103-04A1; Grant sponsor: Whitehall Foundation; Grant number: M20-97; Grant sponsor: NIMH; Grant number: individual National Research Service Award 1 F31 MH12284-01.

*Correspondence to: Leah Krubitzer, Center for Neuroscience, 1544 Newton Court, Davis, CA 95616. E-mail: lakrubitzer@ucdavis.edu

Received 19 September 2000; Revised 22 January 2001; Accepted 22 March 2001

the vestibular nuclei of the brainstem via the dorsal thalamus (Akbarian et al., 1992), is likely to be involved in the sensorimotor integration necessary for these behaviors. Although area 3a has not been systematically described in humans, it has recently been identified in a functional magnetic resonance imaging study as a region rostral to area 3b in which activations are generated in response to deep stimulation (Moore et al., 2000).

Recently, our laboratory has begun to examine area 3a in more detail in both Old World macaque monkeys and New World marmoset monkeys. We have found a number of common features of organization in both primates including a preponderance of neurons responsive to stimulation of deep receptors, an ordered representation of the body surface, and a unique architectonic appearance (Fig. 1; Huffman et al., 1999; Huffman and Krubitzer, 2001). We have extended our studies in marmosets to include the examination of patterns of cortico-cortical and thalamo-cortical connections. The cortical connections of area 3a are distinct from other somatosensory areas in that area 3a receives its densest input from cortical areas associated with the motor system, including the primary (M1), supplementary (SMA), and premotor (PM) areas. Area 3a is also densely interconnected with areas in the posterior parietal cortex (Huffman and Krubitzer, 2001), which is associated with complex behaviors such as goal-directed reaching (Ferraina and Bianchi, 1994; Snyder et al., 1997, 1998; Andersen et al., 1997; for reviews, see Mountcastle et al., 1984; Andersen et al., 2000)

Although the thalamic connections of other anterior parietal fields have been well investigated (Whitsel et al., 1978; Jones et al., 1979; Nelson and Kaas, 1981; Jones and Friedman, 1982; Cusick et al., 1985; Pons and Kaas, 1985; Mayner and Kaas, 1986; Cusick and Gould, 1990; Krubitzer and Kaas, 1992; for reviews, see Jones, 1985; Kaas and Pons, 1988), only a few previous studies in monkeys have examined the thalamo-cortical connections of area 3a. Furthermore, most studies define area 3a by using architectonic criteria alone, which can be problematic (Jones and Porter, 1980). However, these problems can be circumvented when multiple criteria, including electrophysiological recording techniques in combination with studies of architecture, are used to define a cortical field. Previous studies reported that area 3a receives most of its thalamic input from the "shell region" of the caudal division of the ventroposterior lateral nucleus (VPLc; Friedman and Jones, 1981; Darian-Smith and Darian-Smith, 1993), which we believe corresponds to our VPs. However, in the Friedman and Jones (1981) study, injections were made in the thalamus, and the full complement of thalamo-cortical connections of area 3a was not described. In the Darian-Smith and Darian-Smith (1993) study, the area 3a injection sites were not defined electrophysiologically, nor were they always restricted to area 3a. In the only study in primates in which anatomical tracers were injected into electrophysiologically defined locations in area 3a (Akbarian et al., 1992), retrogradely labeled thalamic nuclei included both the oral (VPO or VPo) and superior division of VP (VPs, or "shell" of VPLc).

Although the thalamo-cortical connections of M1 have been described, there are no studies that directly compare the connections of area 3a and M1 in the same animals. The major source of thalamic input to primary motor cortex is from subdivisions of the ventral lateral nucleus (VL or VPLo; Strick, 1975, 1976; Matelli et al., 1989; Holsapple et al., 1991; Darian-Smith and Darian-Smith, 1993; Stepniewska et al 1994a; for reviews, see Jones, 1985, 1998).

In the current investigation we had two goals. The first was to determine the full complement of thalamo-cortical connections of electrophysiologically defined locations in area 3a. The second was to compare thalamic connections of area 3a directly with those of the motor cortex. Our

Abbreviations

Cortical areas and regions	
Cing	cingulate cortex
M1	primary motor area
PM	premotor area
PP	posterior parietal cortex
PV	parietal ventral area
S2	second somatosensory area
SMA	supplementary motor area
Body parts	
ch	chin
dig	digit
fa	forearm
ft	foot
ha	hand
hl	hindlimb
sh	shoulder
tr	trunk
wr	wrist
Direction terms	
di, dist	distal
dor, do	dorsal
glab	glabrous
low	lower
M	medial
pr	proximal
R	rostral
up	upper
ven	ventral
Thalamic nuclei	
AM	anteromedial nucleus
AV	anteroventral nucleus
CL	central lateral nucleus
CM	centre median nucleus
EML	external medullary lamina
F	fasciculus
H	habenular nucleus
LD	lateral dorsal nucleus
LGd	dorsal division of the lateral geniculate nucleus
LP	lateral posterior nucleus
MD	medial dorsal nucleus
Pc	paracentral nucleus
PF	parafascicular nucleus
Pla	anterior pulvinar
Po	posterior nucleus
PUL	pulvinar
R	reticular nucleus
SP	superior pulvinar
St	subthalamic nucleus
TMT	mamillothalamic tract
VA	ventral anterior nucleus
VL	ventral lateral nucleus
VP	ventroposterior nucleus or complex
VPi	ventroposterior inferior nucleus
VPl	ventroposterior lateral nucleus
VPm	ventroposterior medial nucleus
VPs	ventroposterior superior nucleus
ZI	zona inserta
Other	
CP	cerebral peduncle

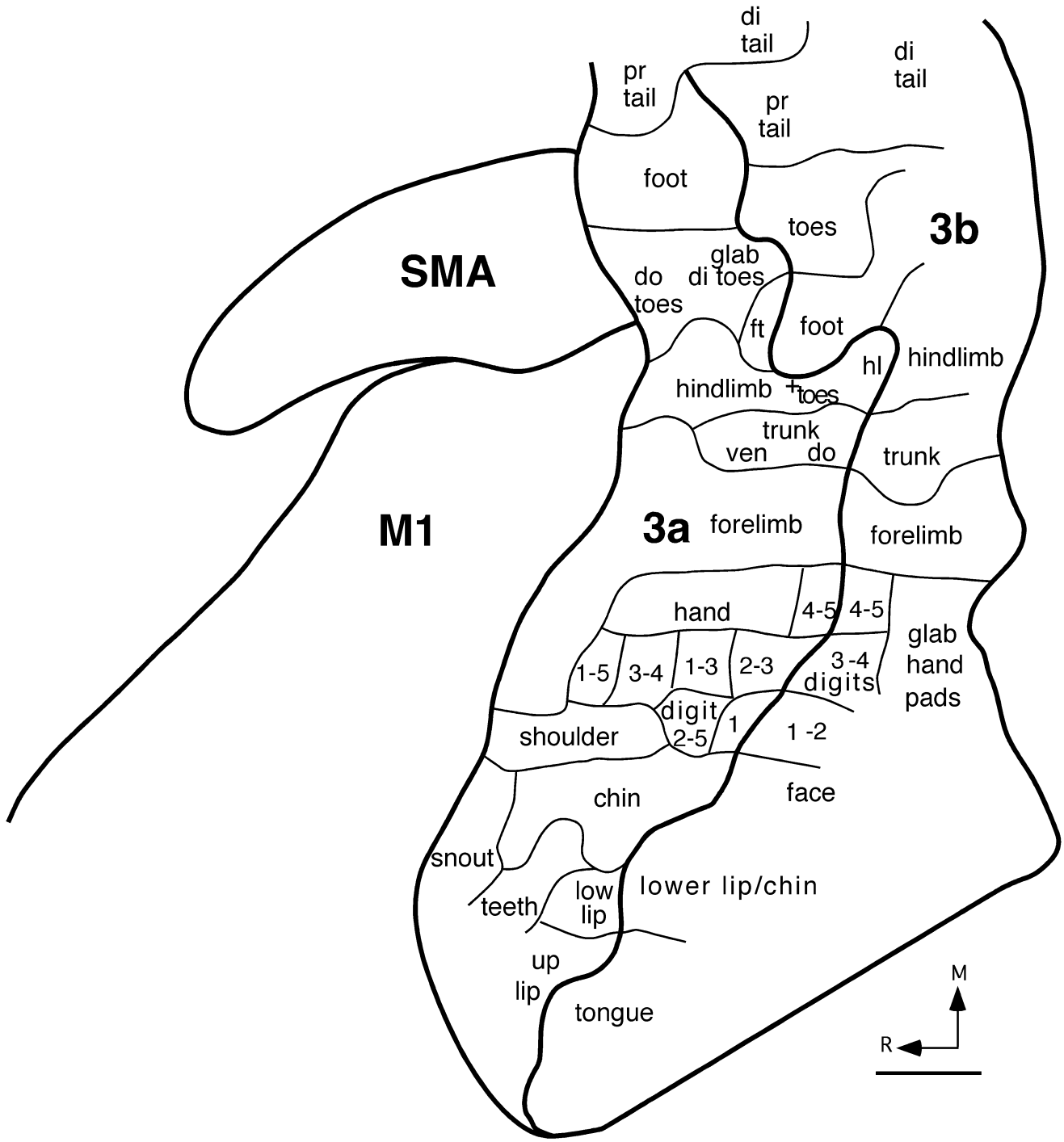

Fig. 1. A map of area 3a and 3b in a flattened left hemisphere. Area 3a is topographically organized with the tail represented most medially, followed by representations of the foot, toes, hindlimb, and trunk. More laterally located are representations of the hand, digits, and face. Thick lines represent cortical boundaries determined from myeloarchitectonic analysis, or myeloarchitectonic and electrophysiological analysis combined. Thin lines mark boundaries between body part representations. (Reproduced with permission from Huffman et al., 2001.) Scale bar = 1 mm.

hypothesis was that, as with cortico-cortical connections, thalamo-cortical connections of area 3a would differ from other anterior parietal somatosensory areas and would have strong interactions with both somatosensory and motor nuclei of the thalamus.

We used the marmoset monkey in the current study for two reasons. First, the marmoset has a nearly lissencephalic cortex, which allows easy access to the field for electrophysiological mapping and injections, whereas the location of area 3a in the macaque monkey is on the

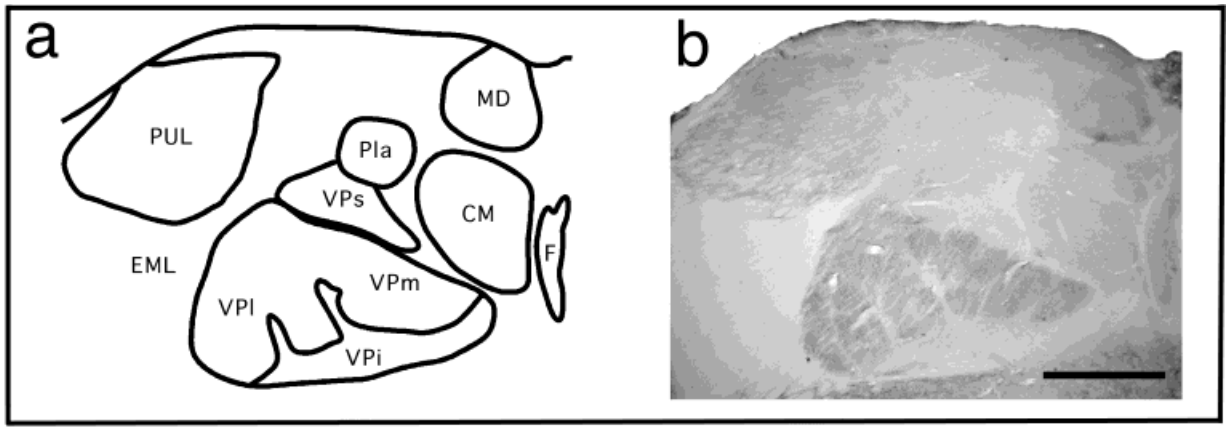

Fig. 2. A reconstruction of nuclear boundaries (**a**) drawn from thalamic sections reacted for CO (**b**), myelin, and Nissl (not shown) in case 96-11. The boundaries of the ventral posterior complex subdivisions (VPl, VPm, VPs, and VPi) can be easily observed. Additionally, the boundaries of MD, CM, and Pla can also be distinguished. By combining nuclear boundaries drawn from the three types of stains, we can accurately determine the location of labeled cell bodies relative to nuclear boundaries. For abbreviations, see list. Dorsal is up, and lateral is to the left. Scale bar = 1 mm.

fundus, and deep in the rostral or caudal bank of the central sulcus (Huffman et al., 1999). The second reason is that much is already known about the organization and connections of the somatosensory cortex and thalamus in the marmoset and the closely related tamarin (Carlson et al., 1986; Krubitzer and Kaas, 1990, 1992; Huffman & Krubitzer, 2001). Thus, the present study is part of a larger effort to fully describe in a single primate the cortical, interhemispheric, and thalamic networks that generate complex manual abilities.

MATERIALS AND METHODS

Anatomical tracing techniques were combined with architectonic analysis to determine the thalamo-cortical connections of area 3a and M1 in four adult marmoset monkeys (*Callithrix jacchus).* Retrograde, and in one case anterograde, patterns of connections were observed by injecting neuroanatomical tracers into electrophysiologically defined body part representations of area 3a, and architectonically defined regions of the M1. In all cases, cortices were removed from the brainstem and thalamus, flattened, and cut tangential to the surface. All injection sites were reconstructed and related to electrophysiological recording results and cortical architecture. The thalami were cut in a coronal plane, and retrogradely labeled cell bodies and anterogradely labeled axon terminals were located and related to architectonically distinct nuclei. All experimental protocols were approved by the Animal Use and Care Administrative Advisory Committee of the University of California, Davis, and conformed to NIH guidelines.

Surgery and injections

Standard sterile surgical procedures were followed in all cases. Each animal was anesthetized with ketamine hydrochloride (30 mg/kg) intramuscularly (IM) and xylazine (2 mg/kg), IM, prior to surgery. Dexamethasone (0.2 mg/kg, IM), and atropine (0.1 mg/kg, IM) were also administered. Additional doses of ketamine hydrochloride (half of initial dose, IM) were administered as needed to maintain a surgical level of anesthesia. Approximately 0.05–0.1 ml of 2% lidocaine was injected subcutaneously near the ear canals where the ear bars were inserted. Heart rate and body temperature were monitored continuously throughout the surgery. The skin was cut, the temporal muscle was retracted, and a craniotomy was made over the somatosensory and motor cortex. Multiunit recording techniques were used to determine the receptive fields (RF) for neurons in area 3a where injections were located. Two injections were centered in the hindlimb representation and two in the forelimb/hand representation. M1 injections were placed rostral to electrophysiologically defined area 3a. A calibrated Hamilton syringe was used to inject 0.3–0.5 μl of 7% Fluoro Ruby (FR), Fluoro Emerald (FE), or 0.03μl of 0.05% wheat germ agglutinin conjugated with horseradish peroxidase (WGA-HRP). Four injections were made in area 3a, and two injections were made in M1. After completion of the injections, a sterile contact lens was placed under the dura, the cut dural flaps were placed over the lens, and the skull opening was covered by a skull cap made of dental acrylic. The cranial muscles and skin were sutured, and each animal was monitored closely during the 2-day (WGA-HRP) or 1-week (FE, FR) recovery period for transport of tracers.

Electrophysiological recordings

Recordings were obtained with low-impedance tungsten-in-glass microelectrodes (0.95–1.5 MΩ at 100 Hz). The electrode was placed perpendicular to the cortical surface; a stepping microdrive was used to advance the electrode to depths of layer IV, 500–700 μm from the pial surface. Once the electrode was in place, the body surface was stimulated, and the RF for neurons at that site was determined and drawn on a picture of the body. Stimulation consisted of displacement of hairs, light brushing of skin surfaces, joint and limb manipulations, pressure, and light to moderate taps. Area 3a was determined electrophysiologically as the region where neurons responded to taps or displacement and manipulation of the limbs. When determining receptive fields for neurons in area 3a, body parts were isolated where possible (such as all portions of

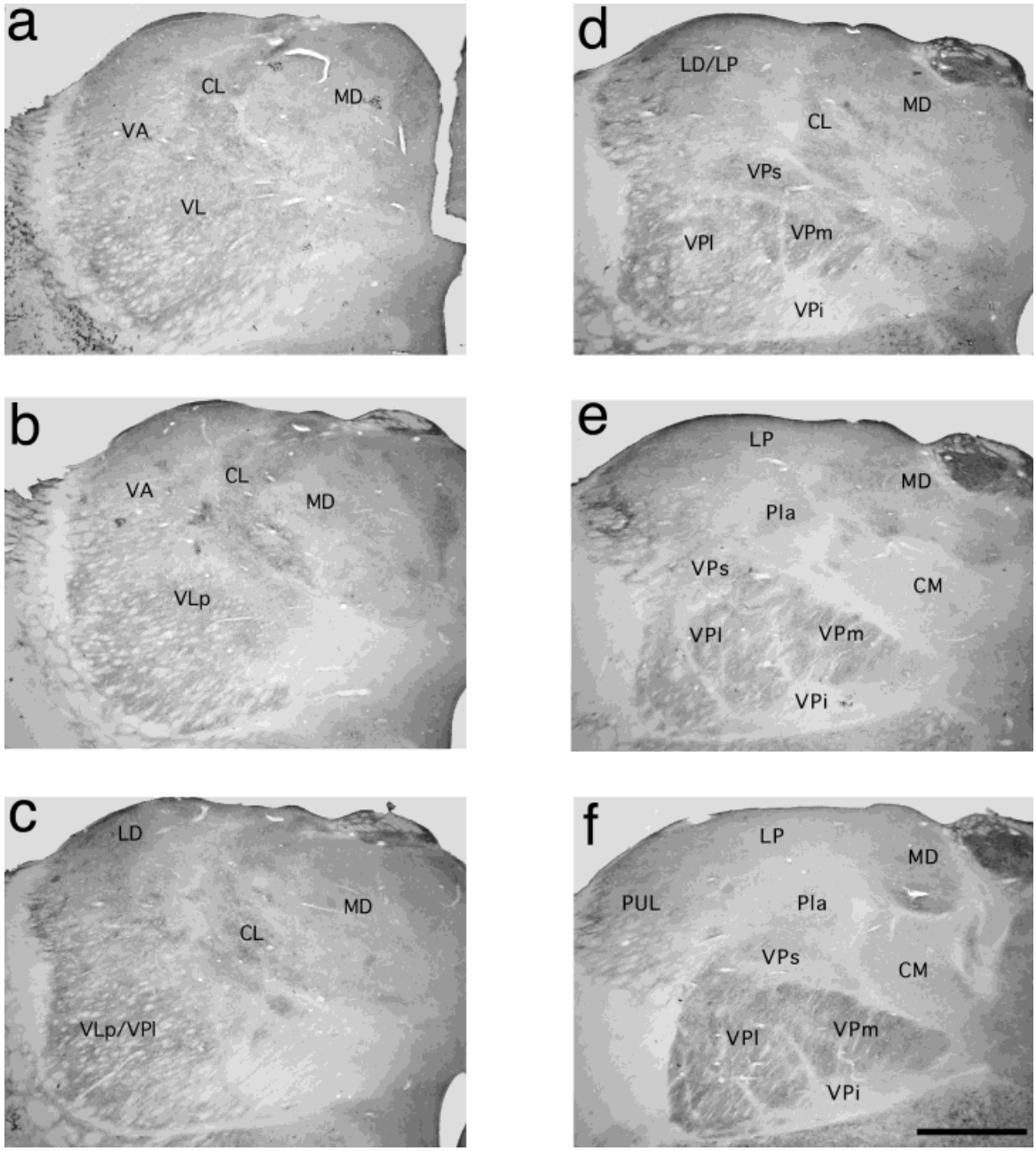

Fig. 3. Lightfield digital images of an anterior-posterior series (a–f) of sections through the thalamus of case 96-11 reacted for CO. At anterior levels of the thalamus, VL (including Vla; a), CL, and MD can be readily identified (**a–c**). With a posterior progression (**d** and **e**), divisions of the ventral posterior nuclear complex are distinct and include VPl, VPm, VPs, and VPi. Far posteriorly (e and **f**), the anterior pulvinar (Pla), and centre-median (CM) nucleus can also be readily identified. These sections are 150 μm apart. Medial is up, and lateral is to the left. For abbreviations, see list. Scale bar = 1 mm.

forelimb and hindlimb). Isolating separate portions of the trunk was difficult. However, upper and lower trunk regions could be isolated.

The types of stimulation required to elicit a response in neurons in area 3a were very different than for neurons in area 3b. Neurons in area 3b required only a very small displacement of hairs or indentation of a small piece of skin to elicit a response, whereas neurons in area 3a required more intense stimulation (light taps), generally over a larger portion of the body surface. Thus, once a portion of the body surface was isolated and joints and limbs immobilized, a small indentation of the skin was insufficient to elicit a neural response in area 3a. Cortical lesions were made at the physiological boundaries of area 3a (10 μA for 10 seconds) for later identification in histologically processed tissue. Also, probes (pasta) were inserted in the cortex at the boundaries of the somatosensory cortex to aid in reconstructing electrophysiological

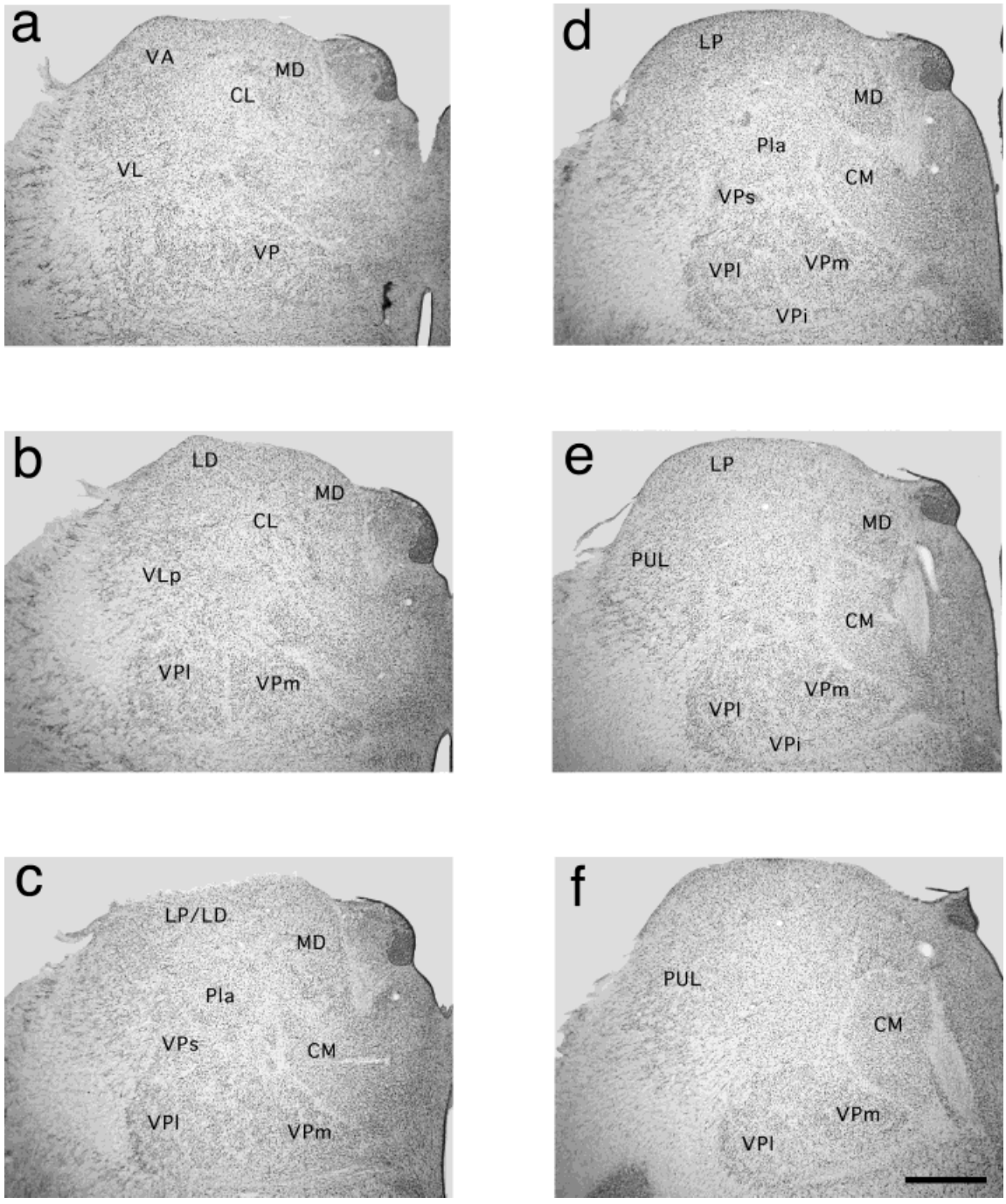

Fig. 4. Lightfield digital images of an anterior-posterior series (a–f) of sections through the thalamus of case 96-8 stained for Nissl. At anterior levels of the thalamus, the anterior portions of the VL (including Vla; a) can be identified, as can MD and CL (**a–c**). With a posterior progression (**d–f**), divisions of the ventral posterior nuclear complex are distinct and include VPl, VPm, VPs, and VPi. The anterior pulvinar (Pla), and centre-median (CM) nucleus can also be identified. Conventions as in previous figures.

and anatomical data. Physiological boundaries were defined by reversals in receptive field progressions, a change in stimulus preference from cutaneous in area 3b, to deep in area 3a, to no response in M1, and by changes in receptive field size (Huffman and Krubitzer, 2001). Physiological results were correlated with architectonic boundaries, and injection sites were drawn from histologically processed tissue (see data analysis below).

Histological processing

After a one week recovery period for the transport of fluorescent tracers and a 2-day recovery period for the

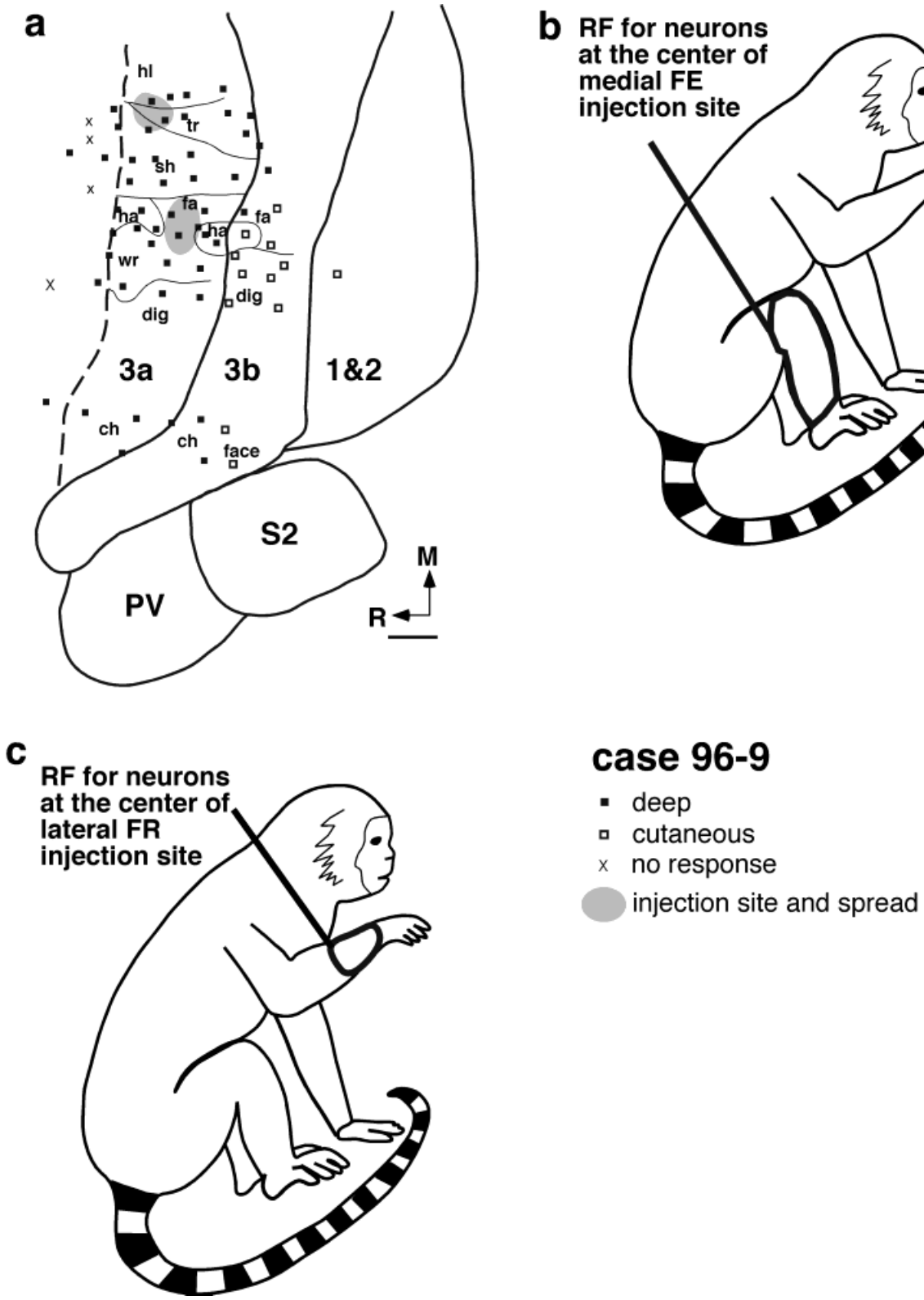

Fig. 5. A partial map of area 3a that depicts the center of two injection sites and their spread in relation to electrophysiologically defined body part representations in case 96-9. **a:** An injection of Fluoro Emerald (FE) was centered in the representation of the hindlimb but spread into the trunk and slightly into the shoulder representations (medial injection site). An injection of Fluoro Ruby (FR) was centered in the representation of the forearm but spread into the wrist representation (lateral injection site). **b,c:** The corresponding receptive fields (RF) for neurons in area 3a in which the FE (b) and FR (c) injections were centered. Solid squares represent electrode penetration locations where neurons responded to the stimulation of deep receptors, and open squares represent locations where neurons responded to the stimulation of cutaneous receptors. Thick lines mark architectonic boundaries using both architectonic analysis and electrophysiological analysis, or architectonic boundaries alone (e.g., areas PV, S2, and 1&2). Thin lines mark physiological boundaries, and dotted lines mark estimated cortical field boundaries. Medial is up, and rostral is to the left. Scale bar in a = 1 mm.

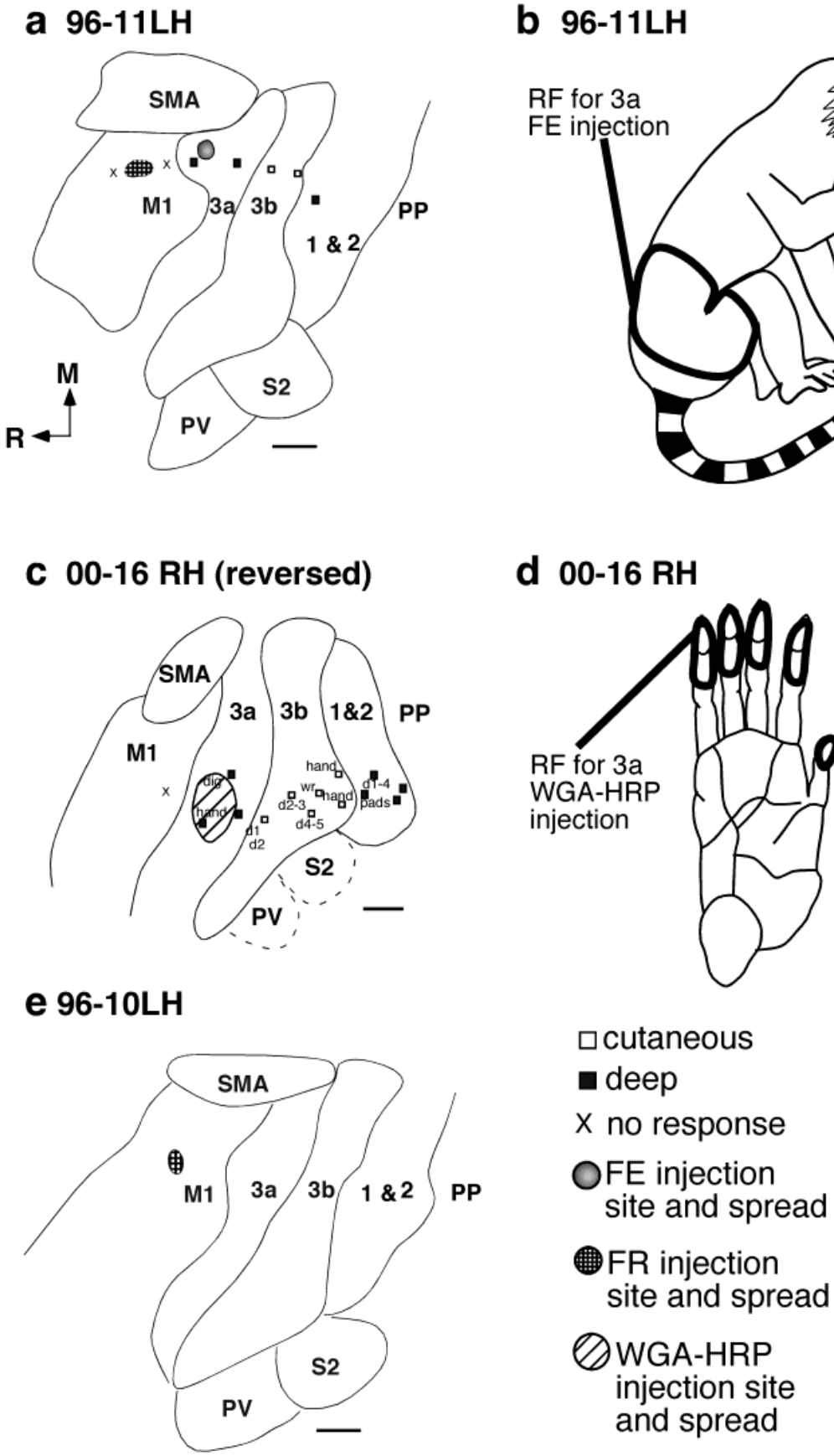

Fig. 6. The location of injection sites (**a**,**c**,**e**) and corresponding receptive fields (RF) for neurons at the sites injected (**b**,**d**) in area 3a. The Fluoro Emerald (FE) injection in 96-11 (a) was centered in area 3a in a location in which neurons responded to stimulation of deep receptors in the proximal hindlimb and adjacent trunk (b). The injection site in area 3a in case 00-16 was centered in a location in which neurons responded to stimulation of deep receptors in the distal digits. In all cases, the injection was restricted to either area 3a or M1. Conventions as in previous figures. FR, Fluoro Ruby; WGA-HRP, wheat germ agglutinin-horseradish peroxidase; LH, left hemisphere; RH, right hemisphere. Scale bar in a = xx, xx in b, c.

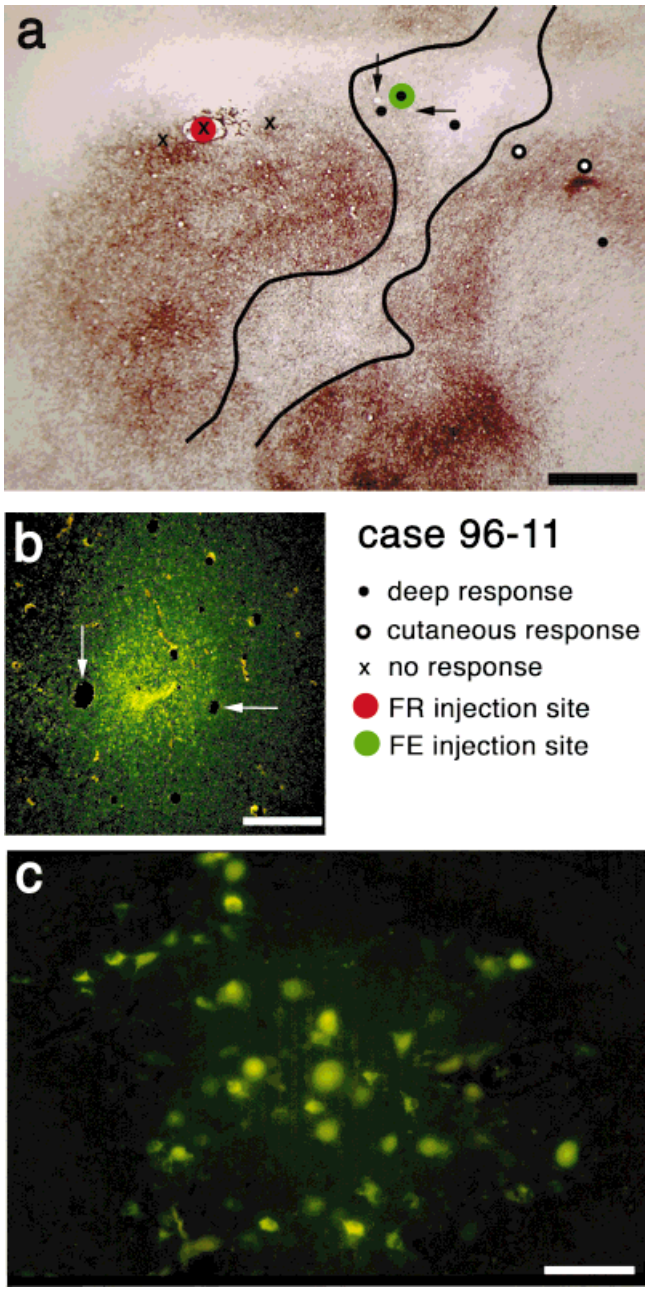

Fig. 7. Digital images of a Fluoro Emerald (FE) injection site centered in the hindlimb representation of area 3a (**a**,**b**), and corresponding retrogradely labeled cells in VPl in the thalamus resulting from that injection (**c**). In a, the FE injection is related to electrophysiological recording and myeloarchitectonic boundaries in a single section. The moderately myelinated area 3a contains neurons that respond to stimulation of deep receptors (filled circles), whereas the darkly myelinated area 3b contains neurons that respond to stimulation of cutaneous receptors (open circles). Neurons in the darkly myelinated M1 were unresponsive to any type of stimulation under our recording conditions. FR, Fluoro Ruby. Arrows in a & b mark the same blood vessels. Scale bars = 1 mm in a; 200 μm in b; 100 μm in c.

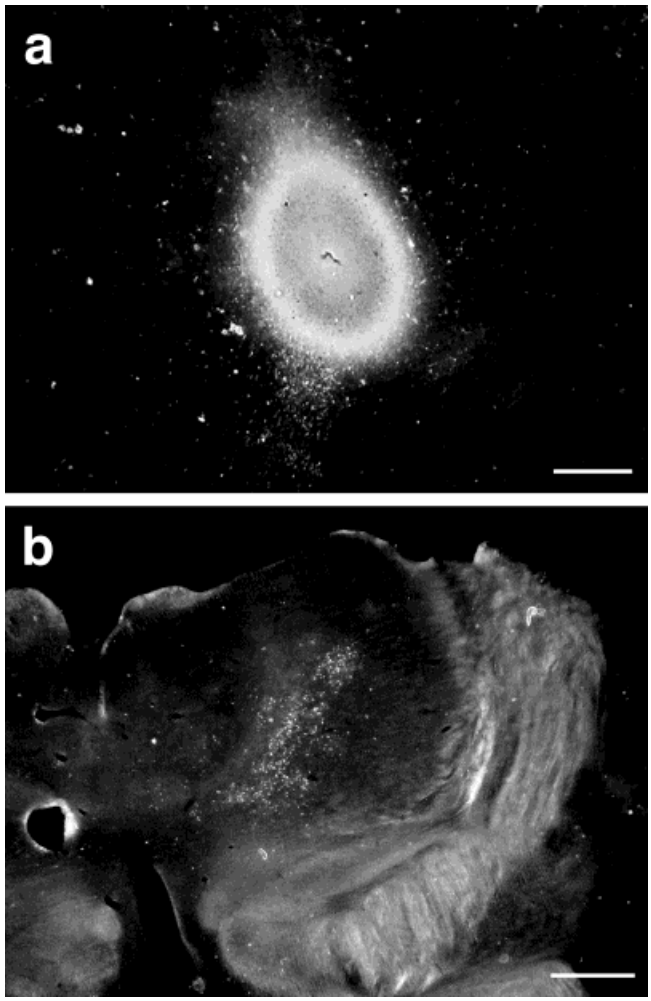

Fig. 8. **a:** Digital image of an injection of WGA-HRP in the digit representation in area 3a of case 00-16. **b:** Corresponding labeled cells and axon terminals in the VL, VPs, and CL of the thalamus. In a, rostral is right and medial is up, and in b lateral is right and dorsal is up. Other conventions as in previous figures. Scale bars = 1 mm.

transport of WGA-HRP, the animals were administered a lethal dose (60 mg/kg) of sodium pentobarbital intraperitoneally (IP) and transcardially perfused with 0.9% saline, 2% paraformaldehyde in phosphate buffer (pH 7.4), and 2% paraformaldehyde in 10% sucrose phosphate buffer (SPB). After the brain was removed from the skull, the corpus callosum was cut, each cortical hemisphere was disected from the brainstem and thalamus, the lateral sulcus was opened, the medial wall was retracted, and the cortex was manually flattened and postfixed for 2 days in 2% paraformaldehyde and 30% SPB, pH 7.4. For the WGA-HRP injection, the brain was soaked overnight in 30% SPB. Each flattened cortex was frozen onto a microtome stage and cut tangential to the cortical surface into 40-μm sections. Alternate sections were stained for myelin (Gallyas, 1979), mounted for fluorescent analysis, or reacted for tetramethyl benzidine (TMB). In one case, the cortex was cut parasagittally and stained for Nissl substance and myelin. The cortico-cortical connections determined from these cortical sections have been described in

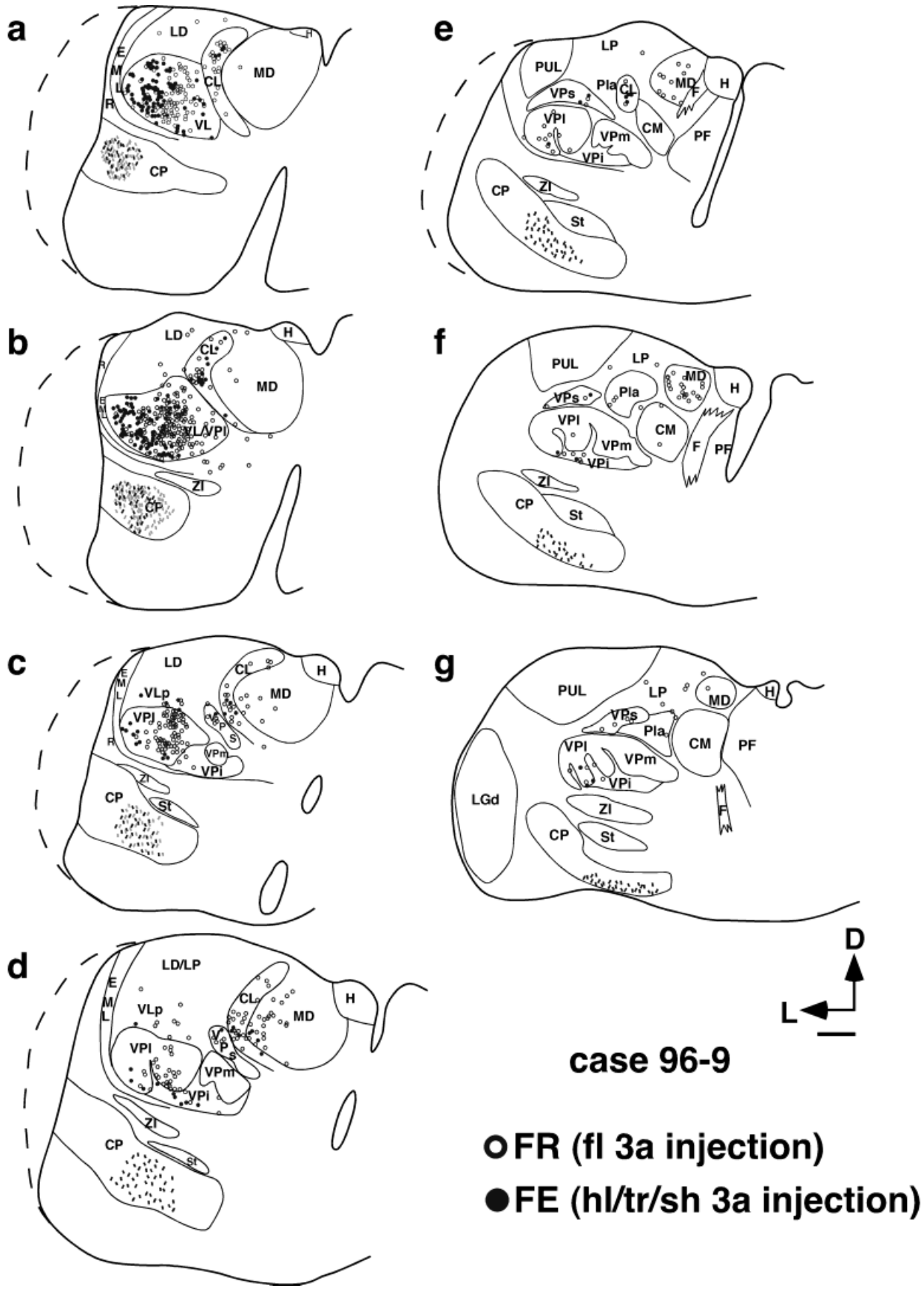
a
LD
E
M
L
R
CL
MD
H
VL
CP
b
LD
CL
H
MD
VL/VPl
ZI
CP
c
LD
E
M
L
VLp
CL
MD
H
VPl
VPm
VPi
ZI
CP
St
d
LD/LP
E
M
L
VLp
CL
MD
H
VPl
VPm
VPi
ZI
CP
St
e
LP
PUL
Pla
CL
MD
H
VPs
VPl
CM
PF
VPm
VPi
CP
ZI
St
f
PUL
LP
MD
H
VPs
Pla
VPl
CM
F
PF
VPm
VPi
ZI
CP
St
g
PUL
LP
MD
H
VPs
Pla
CM
PF
VPl
VPm
VPi
LGd
ZI
F
CP
St
D
L
case 96-9
FR (fl 3a injection)
FE (hl/tr/sh 3a injection)

Figure 9

a different report (Huffman and Krubitzer, 2001). The thalamus was cut coronally on a freezing microtome into 50-μm sections. A one-in-four series of sections was reacted for the mitochondrial enzyme cytochrome oxidase (CO; Carroll and Wong-Riley, 1984), stained for myelin (Gallyas, 1979) or Nissl substance, mounted for fluorescent analysis, or reacted for TMB (Mesulam, 1978, as modified by Gibson et al., 1984).

Data analysis

An imaging system composed of a fluorescent microscope attached to a personal computer equipped with MD-PLOT optical plotting system software (Minnesota Datametrics, St. Paul, MN) was used for data reconstruction. This system was utilized to plot, in X-Y coordinates, the cortical injection sites and spread of the injection, as well as retrogradely labeled cell bodies in coronal thalamic sections. The WGA-HRP injection and transported tracer were reconstructed by using a camera lucida attached to a light microscope. For all cases, the outline of the section, blood vessels, tissue artifacts, lesions, and probes were also drawn for the cortex. In all cases, the injection site and spread was reconstructed, and the myeloarchitectonic boundaries were drawn. Both were related to each other and electrophysiological recording results by matching tissue artifacts and lesions. In this way, the location and spread of the injection site in relation to architectonic and functional boundaries could be determined. For the thalamus, alternate sections stained for Nissl and CO were drawn on a light microscope equipped with a camera lucida. Architectonic boundaries of thalamic nuclei were determined and drawn for every section (Fig. 2). By using blood vessels and artifacts as guides, the labeled cell bodies, and in one case labeled axon terminals, were superimposed onto the architectonic reconstruction of each section. In this way, the exact location of labeled cells and axon terminals could be determined. All sections were drawn at the same magnification in order to facilitate the correlation of the nuclear architecture and the labeled cells (see Fig. 8 for examples of this co-registration). Images of sections through the cortex and thalamus were taken with a Pixera digital camera (Pixera pro and Pixera 120ES, Los Gatos, CA) and were assembled in Adobe PhotoShop 4.0.

Fig. 9. **a–g:** An anterior to posterior reconstruction of sections through the thalamus of case 96-9 (see Fig. 5). The locations of labeled cell bodies, relative to nuclear boundaries, resulting from two area 3a injections are illustrated. Filled circles represent cells labeled with Fluoro Emerald (FE), resulting from an injection into the hindlimb representation in area 3a. Open circles represent cells labeled with Fluoro Ruby (FR), resulting from an injection into the forelimb representation in area 3a. Most of the labeled cells from both injections are in the posterior portion of the ventral lateral nucleus (VL) and the lateral division of the ventral posterior nucleus (VPl). In both the VPl and VL, the topography of connections patterns is evident, with the label from the hindlimb injection located lateral to the label from the forelimb injection. Labeled cells are also observed in the VPs, VPi, Pla, CL, and MD. Small black lines and gray lines in the cerebral peduncle (CP) are portions of labeled axons from the FE and FR injections, respectively. Dorsal is up, and lateral is to the left. Thin lines mark the boundaries of nuclei as determined from Nissl- and CO-stained tissue. These sections are 150 μm apart. The thalamus in this case was slightly torn on the lateral edge, and the dashed line represents the approximate lateral edge of the section. Scale bar = 1 mm.

RESULTS

Electrophysiological recordings and cortical architecture of area 3a

In the present investigation, densely spaced recording sites allowed us to determine a region where most neurons responded to the stimulation of deep receptors. This region, area 3a, contained a complete representation of the deep receptors (Fig. 1). The mediolateral organization of area 3a was similar to area 3b, with the tail represented most medially, followed by the foot and hindlimb representations lateral to the tail representation. The trunk, forelimb, hand, and digit representations were found more laterally, and the representations of the chin, face, and oral structures were in the most lateral position in area 3a.

The physiological borders of area 3a were characterized by changes in the class of receptors stimulated that produced a neural response and reversals in the location of receptive field progression. For example, as recording sites moved from area 3b into area 3a, neurons responded to cutaneous stimulation, and then deep stimulation. As recording sites moved from area 3a to M1, neurons responded to deep stimulation, and then were unresponsive to any type of somatic stimulation in our preparation. In previous evoked potential studies (for review, see Jones and Porter, 1980) and single-unit studies (Tanji and Wise, 1981; Wise and Tanji, 1981), neurons were recorded in M1 that responded to somatic stimulation. The difference in the present investigation and previous investigations was probably due to differences in anesthetic and stimulus paradigm. Reversals in receptive field progression were observed across the 3b/3a border and were also used to delineate area 3a from area 3b. For instance, for the forelimb representation, the locations of receptive fields for neurons changed from the elbow, onto the glabrous hand, digits, and then digit tips in a rostral to caudal progression of recording sites in area 3a. At the 3a/3b border, locations of receptive fields for neurons progressed from the one distal digit tip, onto the proximal digit, then onto the glabrous palm, and finally onto the forearm in a rostral to caudal progression of recording sites in area 3b.

Electrophysiological recordings were related to cortical architecture in tangentially sectioned cortex stained for myelin. To obtain myeloarchitectonic boundaries, the entire series of sections through the flattened cortex was reconstructed and matched with electrophysiological recording results. Area 3b was darkly myelinated and was co-extensive with a complete map of the cutaneous receptors of the body surface. Area 3a was a thin, lightly to moderately myelinated strip of cortex that resided between the more densely myelinated M1 rostrally, and area 3b caudally.

In one case, the cytoarchitecture of area 3a was also examined in parasagittally sectioned cortex stained for Nissl substance. Although no electrophysiological recordings were made in this case, Nissl-stained sections were related to myeloarchitecture so that the cytoarchitectonic boundaries could be indirectly related to physiological results. In Nissl-stained tissue, area 3a contained a thin, granular layer (layer IV), and a prominent layer V with pronounced pyramidal cells. This differed from area 3b, in which a very dense, granular layer is present and layer V is attenuated. The boundary between area 3a and M1 was also apparent. At this boundary, layer IV tapered off into agranular cortex, and layer V contained very large pyra-

midal cells. The electrophysiological results combined with cortical architecture and connections have been described in detail for the marmoset elsewhere (Huffman and Krubitzer 2001).

Architectonic subdivisions of the dorsal thalamus

The ventral posterior nuclear complex and ventral lateral nucleus have been subdivided into different subnuclei by using a variety of methods (Dykes et al., 1981; Jones and Friedman, 1982; Kaas et al., 1984; Jones et al., 1986; Hirai and Jones, 1989; Rausell and Jones, 1991; Stepniewska et al., 1994b; for reviews, see Jones, 1985, 1998). Investigators have subdivided thalamic nuclei differently and/or have used different nomenclature to delineate the same nucleus (see below). In the current study in marmosets, we follow the divisions and nomenclature described in a previous study in marmosets that utilized multiple histochemical staining techniques and patterns of connections to define the subdivisions of VP (Krubitzer and Kaas, 1992). The three divisions of the ventral posterior complex (VPm + VPl, VPi, and VPs; Fig. 2) have distinct cytoarchitectonic appearances, stain differently for the mitochondrial enzyme cytochrome oxidase (CO), and have unique patterns of projections to different areas in the somatosensory cortex. All these nuclear subdivisions, except VPs, conform to those described by Jones (1985, 1998).

In the present investigation, in sections reacted for CO (Figs. 2, 3d–f), the superior (VPs), lateral (VPl), medial (VPm), and inferior (VPi) divisions of VP were clearly distinguished. VPl and VPm, together referred to as VP proper, reacted darkly for CO, whereas VPs reacted moderately and VPi very lightly. Portions of this CO-light VPi interdigitated between different body part representations in VP proper, as described previously by Krubitzer and Kaas (1992). Although not as clear as in the CO-reacted sections, the divisions of VP were observed in sections stained for Nissl (Fig. 4d–f). In these sections, VP proper contained densely packed and darkly stained cells; however, VPi was cell sparse, and cells in VPs were less densely packed and lightly to moderately stained compared with VP.

The ventral anterior nucleus (VA) and the ventral lateral nucleus (VL), which are also a part of the ventral thalamic nuclear group, were distinct in both preparations. VA is located rostral to VL and has been subdivided previously in monkeys (Jones 1985). However, we did not attempt to draw the separate subdivisions. VA reacted moderately for CO (Fig. 3a) and contained large, moderately packed cells that stained darkly for Nissl (Fig. 4a). VL was located posterior to VA and anterior to VP, and the boundary between the VL and VP, and VL and VA was often difficult to distinguish in our coronally sectioned tissue because the boundary between these nuclei lies in a coronal plane (i.e., is parallel to the plane of section). VL has two main divisions, anterior and posterior. While most of VL reacted darkly for CO, in most cases we were able to distinguish the anterior part of VL (Vla; not labeled) by its densely packed small cells, and the posterior portion of VL (VLp) by its larger, less densely packed cells (Fig. 4a,b).

The medial dorsal nucleus (MD), located dorsal to CM and medial to CL, reacted darkly for CO (Figs. 2, 3). MD was a large nucleus that contained fairly evenly spaced, small to medium-sized cells, as appreciated in the sections stained for Nissl (Fig. 4). Although different subdivisions have been described for MD in other primates (Jones, 1985, 1998; Hirai and Jones, 1989), we did not describe these divisions in the marmoset.

Nuclei in the intralaminar group, including the central lateral (CL) and centre median (CM) nuclei, were identified in all cases. CL, which is in the rostral group of the intralaminar nuclei, reacted darkly for CO and contained larger, moderately to darkly stained cells (Figs. 3, 4). CM, which is in the caudal group of the intralaminar nuclei, reacted moderately to darkly for CO and contained tightly packed, small cells (Figs. 2–4). The anterior pulvinar nucleus (Pla) is located between the pulvinar, VP, and CM. Pla reacted lightly to moderately to CO (Figs. 2, 3) and contained small cells that were lightly stained for Nissl (Fig. 4).

Thalamic connections of area 3a

Four injections were placed into area 3a in the left or right hemispheres of three animals. In case 96-9, an FE injection was centered in the representation of the distal hindlimb (Fig. 5a, medial injection site, and 5b) but spread into the neighboring trunk and shoulder representations. In this same case, an FR injection was centered in the representation of the forearm, with some spread into the neighboring hand and wrist representations (Fig. 5a, lateral injection site, and 5c). An injection of FE in case 96-11 was centered in the representation of the hindlimb, with some spread into the trunk representation (Figs. 6a,b, 7a). In the right hemisphere of case 00-16, an injection of WGA-HRP was centered in the representation of the distal glabrous digits (Figs. 6c,d, 8a) and spread into the adjacent representation in which neurons had receptive fields on the entire hand (Fig. 6c).

For each area 3a injection, axon terminals and/or cells were plotted and related to architectonically defined nuclei of the dorsal thalamus. In all cases, most of the labeled cells (and axon terminals in 00-16) were located in the ventral lateral nucleus at the border with the rostral portion of VPl. Indeed, the density of labeled cells and axon terminals in VL, particularly in VLp, far exceeds that found in other thalamic nuclei (Figs. 9–11).The neurons in VL that project to the hand and foot representations in area 3a were topographically organized with those projecting to the foot representation lateral to those projecting to the hand representation.

Labeled cells, and in one case terminals, were also consistently observed in CL. However, in all cases, label was much less dense than in VL (Fig. 10). Labeled cells were also identified in MD. However, the density and consistency of label in this nucleus were low. In one case (00-16), no labeled cells or terminals were identified in MD (Fig. 10), and in two cases (three injections; 96-9 FE and FR; 99-11 FE) only a few cells were observed (Figs. 9, 11).

Labeled cells were observed in several somatosensory nuclei including VPi, VPs, and VPl. In two cases (96-9 FR and 96-11 FE), the labeled cells in VPl were moderately packed (Figs. 9, 11). For two of the injections in area 3a, the number of labeled cells in VPl was much less. For instance, for the FE injection in 96-9, the number of labeled cells in VPl was low, as was the density for case 00-16 (Figs. 9, 10) . Labeled cells and axon terminals were also consistently observed in VPs; in some cases (00-16 and 96-11 FE), the label was dense, whereas in other cases it was moderate (96-9 FR) or sparse (96-9 FE). For three

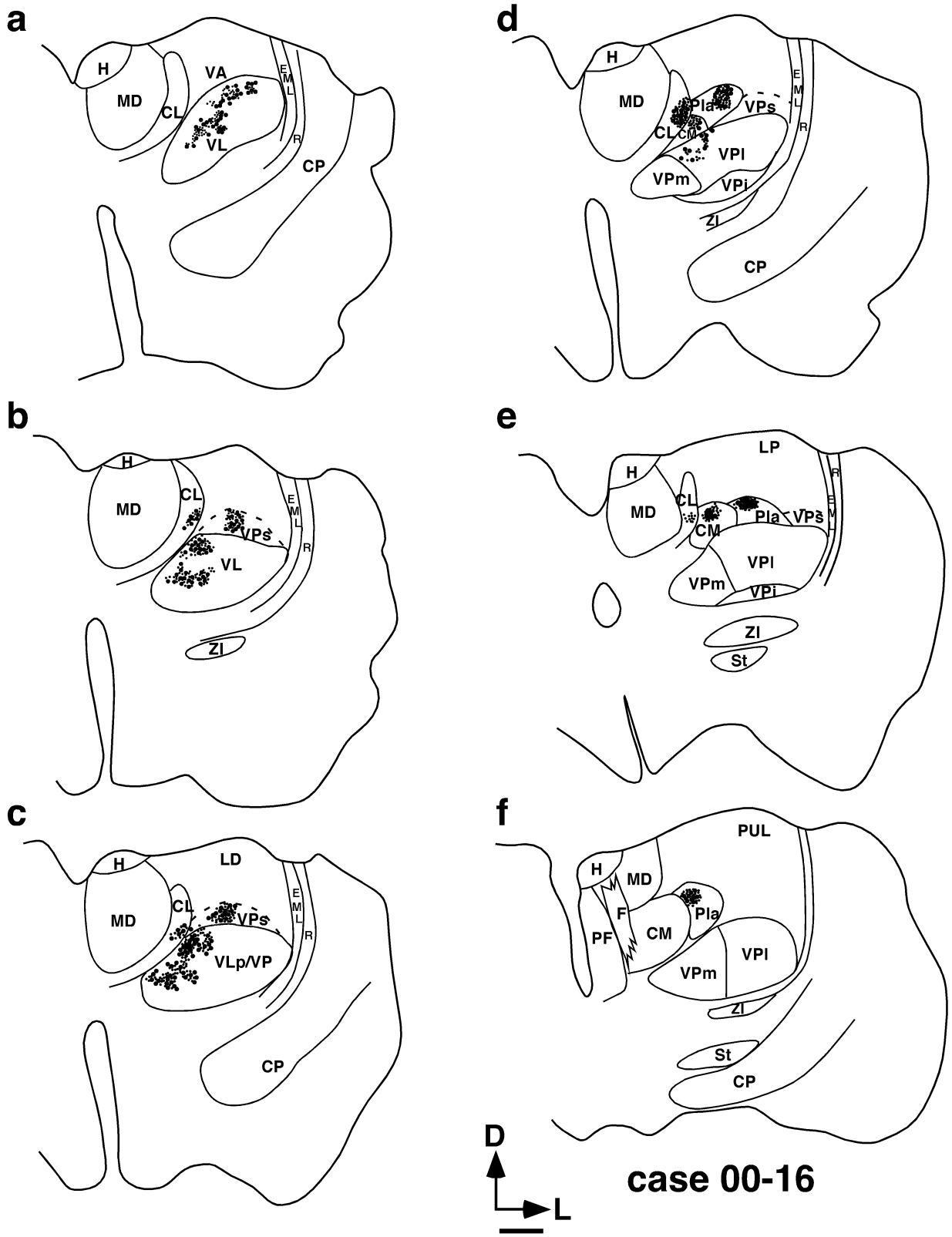

Fig. 10. **a–f:** An anterior to posterior reconstruction of sections through the thalamus of case 00-16 (see Fig. 6c,d) and the locations of labeled cell bodies (large dots) and axon terminals (small dots), relative to nuclear boundaries, resulting from a WGA-HRP injection in the digit representation in area 3a. Most of the labeled cell bodies and axon terminals are located in the ventral lateral nucleus and the rostral portion of VPl. Label is also observed in VPs, Pla, CL, and CM. Conventions as in previous figure. Scale bar = 1 mm.

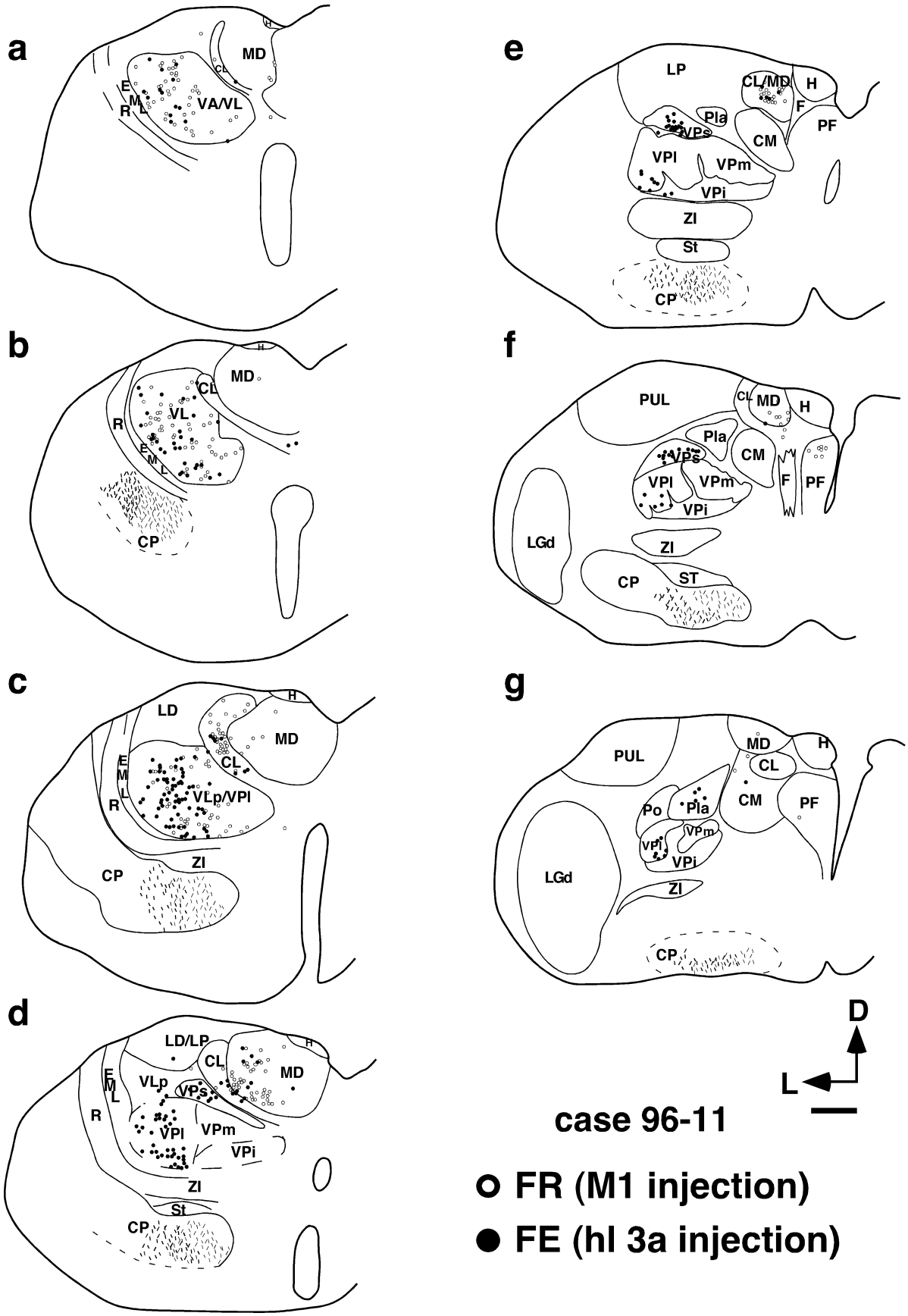

Fig. 11. **a–g:** An anterior to posterior reconstruction of sections through the thalamus of case 96-11 (see Figs. 6a,b, and 7) and the locations of labeled cell bodies, relative to nuclear boundaries, resulting from a Fluoro Emerald (FE) injection in the representation of the hindlimb in area 3a (filled circles), and an injection placed at a similar mediolateral location in M1 (open circles). The densest label resulting from the area 3a injection is in the VL and VPl, with sparse label in VPs, VPi, Pla, CL, and MD. The labeled cell bodies resulting from an injection in M1 are predominantly in VL, VA, CL, and MD. FR, Fluoro Ruby. Conventions as in previous figures. Scale bar = 1 mm.

injections (Figs. 9, 11), a few labeled cells were observed in VPi, and in one case (Fig. 10), no label was observed in VPi**.** However, the lack of label in the three cases may be due to the rather large spacing between sections reconstructed for cell borders and the relatively small size of VPi. In the cases in which the forelimb representation was injected, label tended to be located in the medial aspect of VPl (Figs. 9 [FR], 10), and in cases in which the hindlimb representation was injected, label tended to be in the lateral aspect of VPl (Figs. 9–11).

In three cases, labeled cells and axon terminals were identified in the anterior pulvinar, but in two cases, the density of cells in this nucleus was low (Figs. 9–11). A few cells were identified in one case in the lateral posterior nucleus and lateral dorsal nucleus.

Thalamic connections of M1

Two injections placed in M1 revealed highly consistent patterns of labeled cells in the thalamus. The majority of cells were in VL and VA (Figs. 11 [FR], 12). The other nuclei that were consistently labeled and contained a relatively large number of labeled cells included CL and MD (Figs. 11 [FR], 12). Only a few labeled cells were inconsistently identified in other thalamic nuclei such as CM, Pla, parafascicular nucleus (PF), and anteroventral nucleus (AV). No labeled cells were observed in any of the divisions of the ventral posterior complex after injections in M1.

DISCUSSION

In the present study, neuroanatomical tracers were placed into electrophysiologically defined body part representations of area 3a and architectonically defined locations of M1 to determine the thalamic input to these regions. There were two major findings. First, the majority of thalamic input to area 3a was from a constellation of nuclei classically associated with the motor system, whereas many fewer projections arose from somatosensory nuclei of the ventral posterior complex. Second, M1 had connections with VL, VA, CL, and CM but did not receive input from the ventroposterior nuclear complex (Fig. 13). Although a number of studies have examined thalamo-cortical connections of somatosensory cortex in other species such as cats and some rodents, we have limited our discussion to studies in primates because the morphological structure of the hand and features of organization regarding sensorimotor integration necessary for fine manual discrimination and coordination are likely to be found predominantly in the primate lineage.

Thalamo-cortical connections of area 3a

Reports of thalamo-cortical connections of area 3a in primates vary considerably. Previous anatomical studies in Old World macaque monkeys demonstrated that area 3a had connections predominantly from the shell region of VPlc (Jones et al., 1979; Darian-Smith and Darian-Smith, 1993), which we believe corresponds to our VPs. In addition, one of these studies (Darian-Smith and Darian-Smith, 1993) also described connections with CM, VPLo (our VL), and Pulo (our Pla). Unlike the present investigation in marmosets, these studies do not report connections with any of the divisions of the ventral posterior complex other than the shell of VPLc (VPs). Studies in New World monkeys (such as squirrel monkeys) in which the border zone of area 3a/3b was injected demonstrated connections with VPl, VPs, and Pla, as in the present investigation (Cusick et al., 1985). No connections between area 3a and the motor nuclei of the thalamus were described. Investigations of thalamo-cortical connections of area 3a in squirrel monkeys, which most closely correspond to our study in both methods and results, were those of Akbarian et al. (1992). In these studies, electrophysiologically identified head and neck representations of area 3a were injected, and thalamic connections were observed predominantly with VPO. We do not designate a VPO in the marmoset, but the location and preponderance of retrogradely labeled cells in VPO following 3a injections suggests that it corresponds to our posterior VL. These investigators also describe consistent connections with CL, CM, and PUo (which corresponds to our Pla). Finally, connections were observed with divisions of the ventral posterior complex including VP proper, VPs, and VPi. Overall, despite some differences in nomenclature, the patterns of thalamic label in the Akbarian et al. (1992) study are similar to those reported in the present investigation.

Studies in which electrophysiologically defined locations in the thalamus were injected lend support to the studies described above. In an early study in which injections were placed into electrophysiologically defined locations in the shell region of VPLc (our VPs), dense projections to area 3a were demonstrated (Friedman and Jones, 1981); however, injections into VPLo (our posterior VL) did not result in label in area 3a as in the present investigation. Investigations by Jones and Friedman (1982), in which injections were placed into the ventral posterior nucleus proper (core), demonstrated sparse connections with area 3a. In contrast to the Friedman and Jones (1981) study, a more recent investigation in which VPLo was injected (our VLp) describes projections to the anterior bank of the central sulcus, in the location of area 3a (Nakano et al., 1992).

Taken together, most of the data support the notion that the largest input to area 3a is from motor nuclei of the thalamus including VL, CL, and CM. Only the current study and two previous studies (Jones and Friedman, 1982; Akbarian et al., 1992) demonstrate that divisions of the ventral posterior nucleus, other than the shell region of VPLc (our VPs), project to area 3a as well.

Thalamo-cortical connections of M1

The primate motor thalamus consists of nuclei that receive input from deep cerebellar nuclei and the basal ganglia and project to regions of the premotor and motor cortex (see below). These nuclei include VL, VA, MD, and nuclei of the intralaminar group. In the present study in which injections of retrograde fluorescent tracers were placed into M1, the thalamic nuclei VA, VL, CL, and MD provided the majority of thalamic input to M1, and nuclei such as CM, and Pla had sparse and inconsistent projections to M1.

Early anatomical studies of the thalamo-cortical connections of area 4 (Strick, 1975, 1976; Künzle, 1976; Kievet and Kuypers, 1977; Jones et al., 1979) demonstrate that M1 receives its densest input from VPLo (VLp) and CL. In more recent anatomical studies, VLo, VLc, VPLo, and VLm are reported to provide input to M1 (Matelli et al., 1989; Darian-Smith et al., 1990). Studies in owl monkeys by Stepniewska et al. (1994a), in which different movement representations within M1 were injected with fluo-

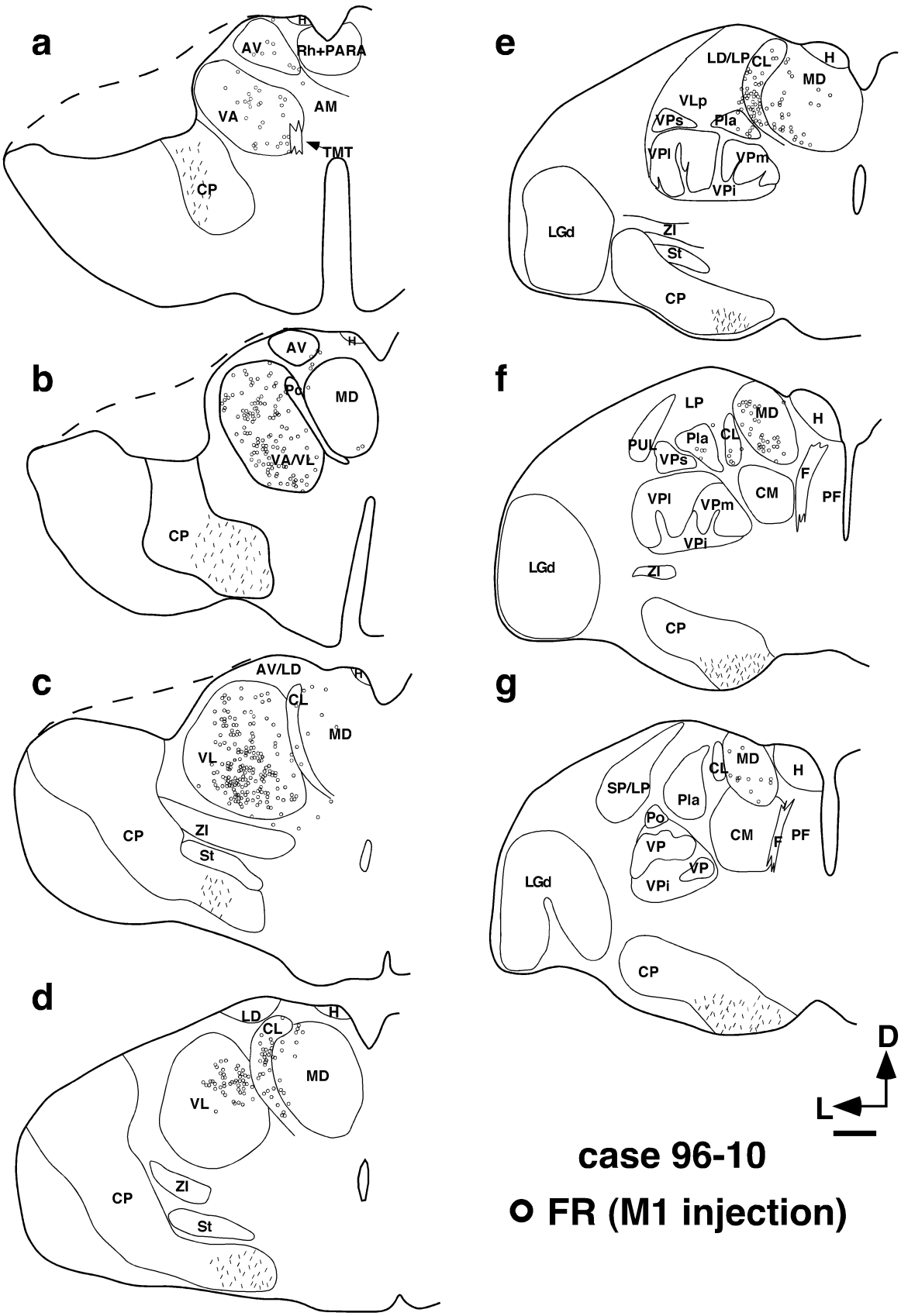

Fig. 12. **a–g:** An anterior to posterior reconstruction of sections through the thalamus of case 96-10 (see Fig. 6e) and the locations of labeled cell bodies (open circles) relative to nuclear boundaries, resulting from an injection in M1. As in the previous case, most of the labeled cells are in VL, VA, CL, and MD. FR, Fluoro Ruby. Conventions as in previous figures. Scale bar = 1 mm.

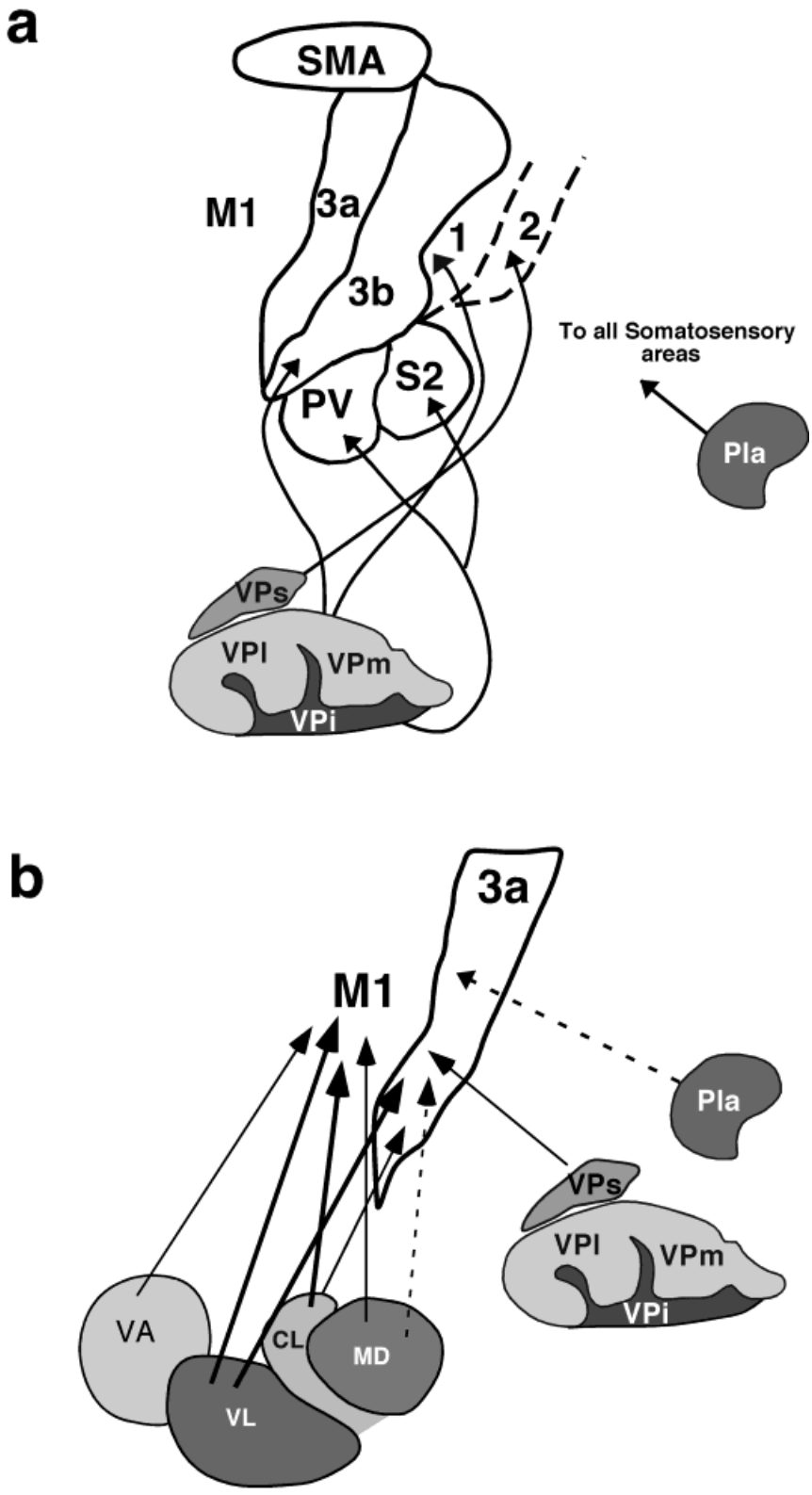

Fig. 13. A summary of the major thalamo-cortical connections of anterior parietal fields in primates (**a**) and our own results for area 3a and M1 (**b**). Whereas somatosensory areas 3b 1, 2, S2, and PV receive their inputs predominantly from nuclei associated with somatosensory processing, area 3a receives most of its input from VL. The thalamic inputs of M1 and area 3a are overlapping to a large extent, with one major difference. Area 3a also receives input from somatosensory nuclei of the thalamus. Thalamo-cortical patterns of connections for area 3b are from Cusick and Gould, 1990, and Krubitzer and Kaas, 1992; those for S2 and PV are from Krubitzer and Kaas, 1992; and those for areas 1 and 2 are from Nelson and Kaas, 1981, and Pons and Kaas, 1985; see also Kaas and Pons, 1988. Conventions as in previous figures.

rescent tracers or WGA-HRP, reported that the strongest projections to M1 were from subdivisions of VL, particularly VLp, and the intralaminar nuclei CL, Pc, and CM. Sparse projections were described from Pla, and a few retrogradely labeled cells were found just inside the lateral border of MD as well. Studies in macaque monkeys in which different movement representations in M1 were injected with neuroanatomical tracers yielded similar results in that the major source of thalamic input to M1 was from VLo and VPLo (Holsapple et al., 1991; Rouiller et al., 1998), which correspond to VLa and VLp, respectively (Jones, 1998).

Studies in which injections were placed in different motor nuclei of the thalamus lend support to the studies described above. For instance, injections in VPLo (our VL) and VA result in dense projections to M1 (Nakano et al., 1992). All studies are consistent with the notion that VLp (VPLo) and CL provide the major source of thalamic input to M1. Unlike area 3a, M1 does not receive cutaneous inputs from any nuclei of the thalamus in either New or Old World monkeys.

Sources of variability across studies

Although we have tried to distill across data sets the major sources of input to area 3a, a good deal of variability exists in the description of thalamo-cortical connections of area 3a. This variability stems from several possible sources. First, access to area 3a is different in different primates. In some primates in which the brain is gyrencephalic, such as macaque monkeys, area 3a lies on the fundus of the central sulcus, or deep in the rostral or caudal bank of the central sulcus. Thus, the placement of injections by using sulcal patterns alone can be highly problematic because the position of electrophysiologically identified area 3a can vary dramatically (Huffman et al., 1999). For example, in a recent investigation in which injections of area 3a were placed relative to sulci and later identified architectonically, only four of 36 injections were restricted to area 3a (Darian-Smith and Darian-Smith, 1993).

A second and related source of variability is in the description or determination of area 3a by different investigators. Jones and Porter (1980) thoroughly outline the difficulties in defining area 3a, as well as the varying descriptions of area 3a in early investigations. They conclude that area 3a in macaque monkeys can be defined as the region immediately rostral to area 3b that has a thinned internal granule cell layer. They felt that the presence or absence of giant pyramidal cells was not a reliable indicator of area 3a. Because of this uncertainty, it would seem that the best way in which to define area 3a is to utilize electrophysiological recording techniques. In both the marmoset (Huffman and Krubitzer, 2001) and macaque monkey (Huffman et al., 1999), in which electrophysiological recording techniques were used, the region of the cortex with an attenuated layer IV (on which a prominent layer V was overlapping) was coextensive with cortex in which neurons were responsive to stimulation of deep somatosensory receptors, such as muscle spindles. In two studies in New World monkeys in which electrophysiological recordings were used to define area 3a, very similar patterns of thalamo-cortical connections were observed (present investigation and Akbarian et al., 1992).

In addition to the differences in the definition of area 3a by different investigators, there are also differences in how the thalamus is subdivided. Classic definitions of the ventral posterior complex and surrounding nuclei rely almost exclusively on cytoarchitectonic distinctions. The ventral posterior nuclear complex is traditionally divided into a central cutaneous core region (VP proper, which is comprised of VPl and VPm), and a shell region (VPLc shell) in which neurons respond to stimulation of deep receptors (Mountcastle and Henneman, 1952; Loe et al., 1977; Jones and Friedman, 1982; Kaas et al., 1984, see Kaas and Pons, 1988 for review). However, electrophysiological recording studies combined with architectonic analysis and/or connections in both New (Kaas et al., 1984, Krubitzer and Kaas, 1992) and Old World monkeys (Krubitzer et al., 1995) demonstrate that the shell region should be considered as a separate nucleus, VPs, which receives input from deep receptors, such as muscle spindles (Krubitzer et al., 1995). Furthermore, VPi, which lies immediately ventral to VPm and VPl, also contains an additional map of deep receptors and should also be considered as a separate nucleus. Thus, the "shell" region of early studies corresponds to two separate nuclei, VPs and VPi, that surround the cutaneous ventral posterior nucleus. Finally, the location and boundaries of VPLo, VPO, the anterior portion of VPLc, and VLp have sometimes been used interchangeably and at other times have been designated as separate nuclei of the thalamus in the same animal. All of these nuclei reside in a similar location in the thalamus, have a similar, although not particularly distinct architectonic appearance, and have been considered to provide the major input to area 3a. Because of these similarities, we believe that these nuclei should be considered as one single nucleus (VLp), until more conclusive data are gathered to suggest otherwise.

The final source of variability of connections of area 3a may be that there is true species variability. However, because of the other sources of variability described above, species differences are extremely difficult to ascertain.

What does area 3a do?

The connections and response properties of neurons in different nuclei in the thalamus that project to area 3a fit well with its suggested role in somato-motor integration, proprioception, and reaching. Neurons that comprise the ventral posterior nuclear complex respond to stimulation of both cutaneous and deep receptors in the skin, muscle, and joints. Specifically, neurons in VP proper respond to cutaneous and low-threshold mechanosensory stimulation (Mountcastle and Henneman, 1952; Loe et al., 1977; Jones and Friedman, 1982; Kaas et al., 1984; Krubitzer and Kaas, 1995; for review, see Kaas and Pons, 1988). Neurons in VPs or the dorsal "shell" of VP respond to stimulation of deep receptors (Jones et al., 1982; Krubitzer et al., 1995), as does the rostral portion of the ventral posterior nucleus (Loe et al., 1977) and the lateral portion of VPLc at the VPLo/VPLc border (Jones et al., 1982). VPs, or a nucleus in the location of VPs also receives inputs from the semicircular canals via the medial vestibular nucleus (Lang et al., 1979). VPi contains neurons that respond to stimulation of Pacinian receptors (Dykes et al., 1981) and deep receptors (Krubitzer et al., 1995). The sources of input to these thalamic nuclei have been well studied and include inputs from the dorsal column nuclei, the main sensory trigeminal nuclei, the lateral cervical nucleus, and the spinothalamic tract (for review, see Kaas and Pons, 1988).

Area 3a also receives input from nuclei of the thalamus classically associated with the motor system (VL, CL CM, and MD). Pallidal connections have been observed with CM (Kuo and Carpenter, 1973; Kim et al., 1976), and the deep cerebellar nuclei project to CL (Asanuma et al., 1983), which in turn projects to area 3a. CL may also be providing nociceptive inputs to area 3a. This is supported by a study in squirrel monkeys, which demonstrates a neural response in area 3a to heat stimulation (Tommerdahl et al., 1996). The types of inputs to VL are varied. For instance, VL receives substantial input from a number of motor structures including the primary motor cortex (Jones et al., 1979), the globus pallidus (Kuo and Carpenter, 1973; Kim et al., 1976; Devito and Anderson, 1982; Parent and DeBellefeuille, 1982; for review, see Mink, 1999), and the cerebellar nuclei (Asanuma et al., 1983; for review, see Bastian et al., 1999). The cerebellum receives proprioceptive inputs from the dorsal and ventral spinocerebellar tract and the external arcuate nucleus, as well as inputs from the vestibular nuclei (for review, see Thach et al., 1992; Bastian et al., 1999). These inputs may be relayed to area 3a via the dentate nucleus of the cerebellum/VL pathway. The dentate nucleus, when lesioned, produces deficits in reaching and pinching (Thach et al., 1992), which fits well with the notion that area 3a is involved in goal-directed reaching.

Thus, area 3a has access to somatic inputs, particularly from muscle spindles via VPs, VLp, and CL of the thalamus, and vestibular inputs via VPs and VLp. In addition, area 3a is part of a motor network that includes the cerebellum, globus pallidus, and motor cortex via its connections with VLp, CM, and CL. Our data clearly suggest that area 3a is not only a somatosensory cortical area, receiving its input from the somatosensory thalamus, but may also be an important cortical component of a network involved in generating a sense of the position of the limbs in space, rotation of the head and neck, and the fine motor movements necessary for reaching and grasping.

ACKNOWLEDGMENTS

We thank Elizabeth Disbrow and Gregg Recanzone for helpful comments on this manuscript. We also thank Debra Hunt and Evan Litinas for photographing Figures 2–4, revising Figure 7, and final manuscript preparation. L.K. was the recipient of grants from the NIH (1 RO1 NS35103-04A1) and the Whitehall Foundation (M20-97). K.J.H. was the recipient of an NIMH individual National Research Service Award (1 F31 MH12284-01).

LITERATURE CITED

Akbarian S, Grüsser OJ, Guldin WO. 1992. Thalamic connections of the vestibular cortical fields in the squirrel monkey (*Saimiri sciureus*). J Comp Neurol 326:423–441.

Andersen RA, Snyder LH, Bradley DC, Xing J. 1997. Multimodal representation of space in the posterior parietal cortex and its use in planning movements. Annu Rev Neurosci 20:303–330.

Andersen RA, Batista AP, Snyder LH, Buneo CA, Cohen YE. 2000. Programming to look and reach in the posterior parietal cortex. In: Gazzaniga MS, editor. The new cognitive neurosciences. Cambridge: The MIT Press. pp 595–524.

Asanuma C, Thach WT, Jones EG. 1983. Distribution of cerebellar terminations and their relation to other afferent terminations in the ventral lateral thalamic region of the monkey. Brain Res Rev 5:237–265.

Bastian AJ, Mugnaini E, Thach WT. 1999. Cerebellum. In: Zigmond MJ, Bloom FE, Landis SC, Roberts JL, Squire LR, editors. Fundamental neuroscience. San Diego: Academic Press. p 973–992.

Carlson M, Huerta MF, Cusick CG, Kaas JH. 1986. Studies on the evolution of multiple somatosensory representations in primates: the organization of anterior parietal cortex in the New World *Callitrichid, saguinus*. J Comp Neurol 246:409–426.

Carroll EW, Wong-Riley MTT. 1984. Quantitative light and electron microscopic analysis of cytochrome oxidase-rich zones in the striate cortex of the squirrel monkey. J Comp Neurol 222:1–17.

Cusick CG, Gould HJ III. 1990. Connections between area 3b of the somatosensory cortex and subdivisions of the ventroposterior nuclear complex and the anterior pulvinar nucleus in squirrel monkeys. J Comp Neurol 292:83–102.

Cusick CG, Steindler DA, Kaas JH. 1985. Cortico-cortical and collateral thalamo-cortical connections of postcentral somatosensory cortical areas in squirrel monkeys: a double labeling study with radiolabeled wheatgerm agglutinin and wheatgerm agglutinin conjugated to horseradish peroxidase. Somatosens Res 3:1–31.

Darian-Smith C, Darian-Smith I. 1993. Thalamic projections to areas 3a, 3b and 4 in the sensorimotor cortex of the mature and infant macaque monkey. J Comp Neurol 335:173–199.

Darian-Smith C, Darian-Smith I, Cheema SS. 1990. Thalamic projections to sensorimotor cortex in the macaque monkey: use of multiple retrograde fluorescent tracers. J Comp Neurol 299:17–46.

DeVito JL, Anderson ME. 1982. An autoradiographic study of efferent connections of the globus pallidus in *Macaca mulatta*. Exp Brain Res 46:107–117.

Dykes RW, Sur M, Merzenich MM, Kaas JH, Nelson RJ. 1981. Regional segregation of neurons responding to quickly adapting, slowly adapting, deep and Pacinian receptors within thalamic ventroposterior nuclei in the squirrel monkey (*Saimiri sciureus*). Neuroscience 6:1687–1692.

Ferraina S, Bianchi L. 1994. Posterior parietal cortex: functional properties of neurons in area 5 during an instructed-delay reaching task within different parts of space. Exp Brain Res 99:175–178.

Friedman DP, Jones EG. 1981. Thalamic input to areas 3a and 2 in monkeys. J Neurophysiol 45:59–85.

Gallyas F. 1979. Silver staining of myelin by means of physical development. Neurology 1:203–209.

Gibson AR, Hansma DI, Houk JC, Robinson FR. 1984. A sensitive low artifact TMB procedure for the demonstration of WGA-HRP in the CNS. Brain Res 298:235–241.

Guldin WO, Akbarian S, Grusser OJ. 1992. Cortico-cortical connections and cytoarchitectonics of the primate vestibular cortex: a study in squirrel monkeys (*Saimiri sciureus*). J Comp Neurol 326:375–401.

Heath CJ, Hore J, Philips CG. 1976. Inputs from low threshold muscle and cutaneous afferents of hand and forearm to areas 3a and 3b of baboon's cerebral cortex. J Physiol (Lond) 257:199–227.

Hirai T, Jones EG. 1989. A new parcellation of the human thalamus on the basis of histochemical staining. Brain Res Rev 14:1–34.

Holsapple JW, Preston JB, Strick PL. 1991. The origin of thalamic inputs to the hand representation in the primary motor cortex. J Neurosci 11:2644–2654.

Hore J, Preston JB, Cheney PD. 1976. Responses of cortical neurons (areas 3a and 4) to ramp stretch of hindlimb muscles in the baboon. J Neurophysiol 39:484–500.

Huffman KJ, Krubitzer L. 2001. Area 3a: topographic organization and cortical connections in marmoset monkeys. Cereb Cortex, in press.

Huffman KJ, Slutsky DA, Disbrow EA, Kahn DM, Recanzone GH, Krubitzer L. 1999. The topographic organization of somatosensory area 3a in the macaque monkey (*Macaca mulatta*). Soc Neurosci Abstr 25:1116.

Johnson JI. 1990. Comparative development of somatic sensory cortex. In: Jones EG, Peters A, editors. Cerebral cortex. New York: Plenum. p 335–449.

Jones EG, Friedman DP. 1982. Projection pattern of functional components of thalamic ventrobasal complex on monkey somatosensory cortex. J Neurophysiol 48:521–544.

Jones EG. 1985. The thalamus. New York: Plenum Press.

Jones EG. 1998. The thalamus of primates. In: Bloom FE, Fjörklund A, Hökfelt T, editors. Handbook of chemical neuroanatomy: the primate nervous system, part II. New York: Elsevier. p 1–298.

Jones EG, Porter R. 1980. What is area 3a? Brain Res Rev 2:1–43.

Jones EG, Wise SP, Coulter JC. 1979. Differential thalamic relationships

of sensory-motor and parietal cortical fields in monkeys. J Comp Neurol 183:833–882.

Jones EG, Friedman DP, Hendry SC. 1982. Thalamic basis of place- and modality-specific columns in monkey somatosensory cortex: a correlative anatomical and physiological study. J Neurophysiol 48:545–568.

Jones EG, Hendry SHC, Brandon C. 1986. Cytochrome oxidase staining reveals functional organization of monkey somatosensory cortex. Exp Brain Res 62:438–442.

Kaas JH, Pons TP. 1988. The somatosensory system of primates. Comp Primate Biol 4:421–468.

Kaas JH, Nelson RJ, Sur M, Lin C-S, Merzenich MM. 1979. Multiple representations of the body within the primary somatosensory cortex of primates. Science 204:521–523.

Kaas JH, Nelson RJ, Sur M, Dykes RW, Merzenich MM. 1984. The somatotopic organization of the ventroposterior thalamus of the squirrel monkey, *Saimiri sciureus*. J Comp Neurol 226:111–140.

Kievit J, Kuypers HGJM. 1977. Organization of the thalamo-cortical connexions to the frontal lobe in rhesus monkey. Exp Brain Res 29:299–322.

Kim R, Nakano K, Jayaraman A, Carpenter MB. 1976. Projections of the globus pallidus and adjacent structures: an autoradiographic study in the monkey. J Comp Neurol 169:263–290.

Krubitzer LA, Kaas JH. 1990. The organization and connections of somatosensory cortex in marmosets. J Neurosci 10:952–974.

Krubitzer LA, Kaas JH. 1992. The somatosensory thalamus of monkeys: cortical connections and a redefinition of nuclei in marmosets. J Comp Neurol 319:123–140.

Krubitzer LA, Florence SL, Jain N, Kaas JH. 1995. Cortical connections from physiologically defined nuclei of the somatosensory thalamus of macaque monkeys. Soc Neurosci Abstr 21:1757.

Kuo J-S, Carpenter MB. 1973. Organization of pallidothalamic projections in the rhesus monkey. J Comp Neurol 151:201–236.

Künzle H. 1976. Thalamic projections from the postcentral motor cortex in *Macaca fascicularis*. Brain Res 105:253–267.

Landgren S, Silfvenius H. 1969. Projection to cerebral cortex of group I muscle afferents from the cat's hindlimb. J Physiol (Lond) 200:353–372.

Lang W, Büttner-Ennever JA, Büttner U. 1979. Vestibular projections to the monkey thalamus: an autoradiographic study. Brain Res 177:3–17.

Loe PR, Whitsel BL, Dreyer DA, Metz CB. 1977. Body representation in ventrobasal thalamus of macaque: a single-unit analysis. J Neurophysiol 40:1339–1355.

Matelli M, Luppino G, Fogassi L, Rizzolatti G. 1989. Thalamic input to inferior area 6 and area 4 in the macaque monkey. J Comp Neurol 280:468–488.

Mayner L, Kaas JH. 1986. Thalamic projections from electrophysiologically defined sites of body surface representations in areas 3b and 1 of somatosensory cortex of cebus monkeys. Somatosens Res 4:13–29.

Mesulam M. 1978. Tetramethylbenzidine for horseradish peroxidase neurohistochemistry: a noncarcinogenic blue reaction-product with super sensitivity for visualizing afferents and efferents. J Histochem Cytochem 26:106–117.

Mink JW. 1999. Basal ganglia. In: Zigmond MJ, Bloom FE, Landis SC, Roberts JL, Squire LR, editors. Fundamental neuroscience. San Diego: Academic Press. p 951–972.

Moore CI, Stern CE, Corkin S, Fischel B, Gray AC, Rosen BR, Dale AM. 2000. Segregation of somatosensory activation in the human rolandic cortex using fMRI. J Neurophysiol 84:558–569.

Mountcastle VB, Henneman E. 1952. The representation of tactile sensibility in the thalamus of the monkey. J Comp Neurol 97:409–489.

Mountcastle VB, Motter BC, Steinmetz MA, Duffy CJ. 1984. Looking and seeing: the visual functions of the parietal lobe. In: Edelman GM, Cowan WM, Gall WE, editors. Dynamic aspects of neocortical function. New York: John Wiley & Sons. p 159–193.

Nakano K, Tokushige A, Kohno M, Hasegawa Y, Kayahara T, Sasaki K. 1992. An autoradiographic study of cortical projections from motor thalamic nuclei in the macaque monkey. Neurosci Res 13:119–137.

Nelson RJ, Kaas JH. 1981. Connections of the ventroposterior nucleus of the thalamus with the body surface representations in cortical areas 3b and 1 of the cynomologus macaque, *Macaca fascicularis*. J Comp Neurol 199:29–64.

Nelson RJ, Sur M, Felleman DJ, Kaas JH. 1980. Representations of the body surface in postcentral parietal cortex of *Macaca fascicularis*. J Comp Neurol 192:611–643.

Oscarsson O, Rosen I. 1966. Short-latency projections to the cat's cerebral cortex from the skin and muscle afferents in the contralateral forelimb. J Physiol 182:164–184.

Parent A, DeBellefueuille L. 1982. Organization of efferent projections from the internal segment of globus pallidus in primate revealed by fluorescence retrograde labeling method. Brain Res 245:201–213.

Phillips CB, Powell TPS, Wiesandanger M. 1971. Projections from low threshold muscle afferents of hand and forearm to area 3a of baboon's cortex. J Physiol 217:419–446.

Pons TP, Kaas JH. 1985. Connections of area 2 of somatosensory cortex with the anterior pulvinar and subdivisions of the ventroposterior complex in macaque monkeys. J Comp Neurol 240:16–36.

Pons TP, Garraghty PE, Cusick CG, Kaas JH. 1985. The somatotopic organization of area 2 in macaque monkeys. J Comp Neurol 241:445–466.

Rausell E, Jones EG. 1991. Histochemical and immunocytochemical compartments of the thalamic VPM nucleus in monkeys and their relationship to the representational map. J Neurosci 11:210–225.

Rouiller EM, Tanne J, Moret V, Kermadi I, Boussaoud D, Welker E. 1998. Dual morphology and topography of the corticothalamic terminals originating from the primary, supplementary motor, and dorsal premotor cortical areas in macaque monkeys. J Comp Neurol 396:169–185.

Snyder LH, Batista AP, Andersen RA. 1997. Coding of intention in the posterior parietal cortex. Nature 386:167–170.

Snyder LH, Batista AP, Andersen RA. 1998. Change in motor plan without a change in the spatial locus of attention modulates activity in posterior parietal cortex. J Neurophysiol 79:2814–2819.

Stepniewska I, Preuss TM, Kaas JH. 1994a. Thalamic connections of the primary motor cortex (M1) of owl monkeys. J Comp Neurol 349:558–582.

Stepniewska I, Preuss TM, Kaas JH. 1994b. Architectonic subdivisions of the motor thalamus of owl monkeys: Nissl, acetylcholinesterase, and cytochrome oxidase patterns. J Comp Neurol 349:536–557.

Strick PL. 1975. Multiple sources of thalamic input to the primate motor cortex. Brain Res 88:372–377.

Strick PL. 1976. Anatomical analysis of ventrolateral thalamic input to primate motor cortex. J Neurophysiol 39:1020–1031.

Sur M, Nelson RJ, Kaas JH. 1980. Representation of the body surface in somatic koniocortex in the prosimian *Galago*. J Comp Neurol 189:381–402.

Tanji J. 1975. Activity of neurons in cortical area 3a during maintenance of steady postures by the monkey. Brain Res 88:549–553.

Tanji J, Wise S. 1981. Submodality distribution in sensorimotor cortex of the unanesthetized monkey. J Neurophysiol 45:467–481.

Thach WT, Goodkin HP, Keating JG. 1992. The cerebellum and the adaptive coordination of movement. Annu Rev Neurosci 15:403–442.

Tommerdahl M, Delemos KA, Vierck CJ Jr., Favorov OV, Whitsel BL. 1996. Anterior parietal cortical responses to tactile and skin-heating stimuli applied to the same skin site. J Neurophysiol 75:2662–2670.

Whitsel BL, Rustioni A, Dreyer DA, Loe PR, Allen EE, Metz CB. 1978. Thalamic projections to S-I in macaque monkey. J Comp Neurol 178: 385–410.

Wise S, Tanji J. 1981. Neuronal responses in sensorimotor cortex to ramp displacements and maintained positions imposed on hindlimb of the unanesthetized monkey. J Neurophysiol 45:482–500.

Yumiya H, Kubota K, Asanuma H. 1974. Activities of neurons in area 3a of the cerebral cortex during voluntary movements in the monkey. Brain Res 78:169–177.